Earth Syst. Dynam., 4, 145–170, 2013
www.earth-syst-dynam.net/4/145/2013/
doi:10.5194/esd-4-145-2013

Earth System Dynamics
Open Access

Simple emission metrics for climate impacts

B. Aamaas, G. P. Peters, and J. S. Fuglestvedt

Center for International Climate and Environmental Research – Oslo (CICERO), PB 1129 Blindern, 0318 Oslo, Norway

Correspondence to: B. Aamaas (borgar.aamaas@cicero.oslo.no)

Received: 31 July 2012 – Published in Earth Syst. Dynam. Discuss.: 30 August 2012
Revised: 25 March 2013 – Accepted: 3 April 2013 – Published: 6 June 2013

Abstract. In the context of climate change, emissions of different species (e.g., carbon dioxide and methane) are not directly comparable since they have different radiative efficiencies and lifetimes. Since comparisons via detailed climate models are computationally expensive and complex, emission metrics were developed to allow a simple and straightforward comparison of the estimated climate impacts of emissions of different species. Emission metrics are not unique and variety of different emission metrics has been proposed, with key choices being the climate impacts and time horizon to use for comparisons. In this paper, we present analytical expressions and describe how to calculate common emission metrics for different species. We include the climate metrics radiative forcing, integrated radiative forcing, temperature change and integrated temperature change in both absolute form and normalised to a reference gas. We consider pulse emissions, sustained emissions and emission scenarios. The species are separated into three types: CO_2 which has a complex decay over time, species with a simple exponential decay, and ozone precursors (NO_x, CO, VOC) which indirectly effect climate via various chemical interactions. We also discuss deriving Impulse Response Functions, radiative efficiency, regional dependencies, consistency within and between metrics and uncertainties. We perform various applications to highlight key applications of emission metrics, which show that emissions of CO_2 are important regardless of what metric and time horizon is used, but that the importance of short lived climate forcers varies greatly depending on the metric choices made. Further, the ranking of countries by emissions changes very little with different metrics despite large differences in metric values, except for the shortest time horizons (GWP20).

1 Introduction

Multi-component climate policies require a method to compare the climate impact of emissions of different species (Fuglestvedt et al., 2003; O'Neill, 2000; Forster et al., 2007). While it is most common to compare different long-lived greenhouse gases (LLGHGs), e.g., CO_2 and CH_4, it may also be useful to compare short lived climate forcers (SLCFs), e.g., black carbon (BC) and organic carbon (OC), and to compare LLGHGs and SLCFs, e.g., CO_2 and BC. Different species have different radiative efficiencies and remain in the atmosphere over different time scales (Forster et al., 2007). Thus, a direct comparison of species by weight does not correlate with the climate impact. As a consequence, emission metrics were developed as a simple means to compare the relative climate impacts of the emission of different species (Wuebbles, 1989; Derwent et al., 1990; Lashof and Ahuja, 1990; IPCC, 1990).

The most straightforward way to compare the impacts of emissions of different components is with Radiative Forcing (RF), and most emission metrics use RF as a starting point. A well-known application of the RF is to compare the RF at two points in time, such as the change in RF between current and pre-industrial times (Forster et al., 2007, Fig. 2.20). Some transient features of the RF can be included by integrating the RF over time leading to the most common method of comparing GHGs, the Global Warming Potential (GWP). The GWP compares the integrated RF of a pulse emission of a given species relative to the integrated RF of a pulse emission of CO_2. The GWP with a 100 yr time horizon is used for reporting of emissions under the UNFCCC and its Kyoto Protocol, and consequently is applied almost universally in life cycle assessment and other forms of GHG reporting at the national, regional, city, industry, and individual levels (Peters, 2010). The GWP was originally proposed

as a "simple approach... to illustrative the difficulties inherent in the concept, to illustrate the importance of some of the current gaps in understanding and to demonstrate the current range of uncertainties" in the IPCC First Assessment Report (IPCC, 1990). It is not entirely clear how the GWP received widespread acceptance given the very cautious nature of its introduction (Shine, 2009) and, perhaps not surprisingly, it has since been critiqued from many angles (Fuglestvedt et al., 2000, 2003; Manne and Richels, 2001; Manning and Reisinger, 2011; Shine, 2009; Victor, 1990; Smith and Wigley, 2000a, b). Most critiques focus on the physical interpretation of the GWP in terms of the climate impact and if this is broadly consistent with the objectives of climate policy.

In response to the critiques of the GWP, several alternatives have been proposed. The Global Temperature change Potential (GTP) (Shine et al., 2007, 2005b) is increasingly applied in the literature, but has yet to be broadly applied for emission accounting or policy applications. The GTP compares the temperature change at a point in time due to a pulse emission of a species i relative to the temperature change due to a pulse emission of CO_2. The GTP combines the temporal change in the RF of different species with the temporal behaviour of the temperature response of the climate system, thus, going beyond a key limitation of the GWP.

Numerous other emission metrics have been proposed (see Tanaka et al., 2010 for a review), but these are in less common usage than the GWP and GTP. Many of the alternative emission metrics are not easily represented in a reduced mathematical form as they depend on inverse modelling (e.g., Wigley, 1998) or economic modelling (e.g., Manne and Richels, 2001). While these more complex emission metrics may give more realistic responses for a given climate impact, they lack the transparency of simple reduced form metrics. Reduced form metrics are generally parameterised with more complex models, and within the range of the parameterisation, are expected to be sufficient for most applications. The definition of "sufficient" depends on criteria for evaluation (O'Neill, 2000), and in this article we limit our discussion to emission metrics that can be easily represented in a reduced mathematical form, while fully acknowledging that alternatives exist. Our aim is to discuss key assumptions and issues in the calculation and use of these reduced form emission metrics.

All of the IPCC Assessment Reports have had a section on emission metrics (IPCC, 1990, 1995, 2001, 2007), and several other IPCC related reports have contributed additional background information (Isaksen et al., 1992; IPCC, 1994, 2009; Enting et al., 1994). In addition to updating the scientific progress on emission metrics, each new IPCC report typically updates radiative efficiencies and atmospheric lifetimes, which are core components of most emission metrics. The motivation for this paper is to present the relevant background, key assumptions, and equations used to estimate common emission metrics. While the metric equations are not new (Fuglestvedt et al., 2010; Peters et al., 2011a), here we combine them together in a consistent framework and provide ancillary information on their interpretation and application. The parameters used in this paper are based on the IPCC Fourth Assessment Report (Forster et al., 2007) for consistency, but as new input becomes available, it is straight forward to update the metric values using the material presented in this paper.

This paper is structured as follows. In Sect. 2, we first give a background overview of emission metrics, followed by a presentation of the key components used to construct emission metrics. Section 3 shows the analytical expressions for common emission metrics. In Sect. 4, some cross-cutting issues relevant for all metrics are presented. Section 5 discusses methods for using metrics in emission scenarios. Section 6 demonstrates the use of emissions metrics in some common applications. We conclude in Sect. 7.

2 Metric overview, key components, and assumptions

Emission metrics have numerous different applications (Fuglestvedt et al., 2003; Tanaka et al., 2010), but the main ones are to (1) provide an "exchange rate" on how to weigh the emissions of different species for mitigation policies, as in the Kyoto Protocol, and to be able to report emission under the UNFCCC (Skodvin and Fuglestvedt, 1997), (2) perform comparisons of different activities and technologies that emit species at different rates such as in Life Cycle Assessment (LCA) (Peters et al., 2011b; Pennington et al., 2004; Boucher and Reddy, 2008; Tanaka et al., 2012), and (3) compare the climate impacts of the emissions of different species to gain greater scientific understanding (e.g., Collins et al., 2010; Shindell et al., 2009). Due to the variety of applications, there is no obvious scientific need to have one single metric for all applications, and a range of different metrics may even be used in one application.

2.1 General structure of a metric

It is worthwhile to start with a general formulation of an emission metric (Kandlikar, 1996; Forster et al., 2007)

$$\mathrm{AM}_i = \int_0^{\mathrm{TH}} \left[\left(I\left(\Delta C_{r+i}\left(t\right)\right) - I\left(\Delta C_r\left(t\right)\right)\right) g\left(t\right) \right] \mathrm{d}t \qquad (1)$$

where $I(\Delta_i(t))$ is a function describing the "impact" of a change in climate (e.g., concentration, temperature, precipitation), ΔC, at time t, with a discount function, $g(t)$, and compared to a reference system, r, on which the perturbation occurs, i. To compare two emission perturbations i and j, the climate impact can be compared as a function of time using $\mathrm{AM}_i(\mathrm{t})$ and $\mathrm{AM}_j(\mathrm{t})$. It is also possible to consider normalised metrics, $M_i = \mathrm{AM}_i/\mathrm{AM}_j$ where j is a reference gas, and M_i compares the climate impact of one species i relative to the reference gas j as in the case of CO_2-equivalent emissions.

The key factors defining a particular emission metric are the impact function I – with key examples including RF, temperature, and damages – and the discount function. The discount function, $g(t)$, is generally considered to be an exponential function, $g(t) = e^{-rt}$, but in emission metrics several alternatives are used, such as no discounting, $g(t) = 1$, step functions for a given time horizon, $g(t \leq \mathrm{TH}) = 1$, $g(t > \mathrm{TH}) = 0$, and instantaneous evaluation at a given time horizon using a Dirac delta function[1], $g(t) = \Delta(t)$. The Ozone Depletion Potential, which serves a similar purpose to the GWP for ozone depletion (IPCC, 1990), did not use any discounting, $g(t) = 1$, in effecting choosing an infinite time horizon (Cox and Wuebbles, 1989). A particular challenge with climate-based emissions metrics is that some sort of discounting is necessary due to the long-term behaviour of CO_2 (Lashof and Ahuja, 1990). Since a pulse emission of CO_2 does not decay to zero, then without discounting, the metric value for CO_2 diverges. The GWP uses a step function for discounting requiring the use of a chosen time horizon (TH) which can take any value between 0 and infinity. Fuglestvedt et al. (2003) replicated GWPs using damage-based metrics with discount rates and found that if a single time horizon is used in the GWP, then this implies different discount rates (for a given damage function) for the various gases. The GTP uses a Dirac delta function as a discount function which evaluates the AM_i at one point in time only (also labeled TH). Several studies have also used a time-varying TH, where the TH changes as it moves towards a target year (TE), TH = TE-t (Shine et al., 2007). The time-varying metric shows the characteristic features of many emission metrics from the economic literature (Manne and Richels, 2001; Johansson, 2012; Reisinger et al., 2013).

We develop the different emission metrics based around the use of Eq. (1). While seemingly abstract, the application of Equation 1 can be applied by following some simple steps, and here we give an illustrative example of concentration and RF. An emission into the atmosphere leads to an increase in the atmospheric concentration of that component. The atmospheric concentration has a "direct" decay dependent on the efficiency that the species is removed from the atmosphere, which is described by an impulse response function (IRF). Due to chemical reactions in the atmosphere, some emissions of one type of component can lead to an "indirect" increase or decrease in the concentration of another type of component (e.g., ozone precursors). While the species is resident in the atmosphere, the direct increase in the atmospheric concentration of the species causes an additional RF, which for emission metrics is usually expressed in a linearized form about a reference concentration (the radiative efficiency). The radiative forcing caused by indirect changes in other species is estimated analogously. The response considered in the metrics is governed by the temporal evolution of the RF, which is dependent on the radiative efficiency and removal rate from the atmosphere leading to $\Delta C(t)$. The impact I can be directly related to the RF through simple climate or economic models, with the discount function putting different weights on different time periods. Each of these steps is described in more detail below.

[1]A Dirac delta function centred at TH, δ(TH), is zero everywhere except for $t = \mathrm{TH}$ and, thus, the impact, $I(\Delta_i(t))$, is evaluated at a single point, $t = \mathrm{TH}$.

Table 1. Parameters used in the metric equations.

Time horizon (years)	H
Radiative efficiency ($\mathrm{W(m^2kg)^{-1}}$); RF due to a marginal increase in atmospheric concentration	A_x
Parameters for the exponential Impulse Response Function (IRF) for atmospheric decay of each species	
Weight on each exponential (unitless)	$a_i, \Sigma a_i = 1$
Decay times of each exponential (years)	τ_i
Number of exponentials (unitless)	I
Parameters of the exponential Impulse Response Function (IRF) of the climate model response to pulse RF	
Components of the climate sensitivity ($\mathrm{K(Wm^2)^{-1}}$)	$c_j, \lambda = \Sigma c_i$
Decay times due to each component of c_i (years)	d_j
Number of decay terms (unitless)	J
Ozone precursor specific parameters	
Radiative efficiency ($\mathrm{W(m^2kg\,yr)^{-1}}$) for perturbation S	A^S_{OP}
Primary mode methane adjustment time (years)	τ_{PM}
Short-lived ozone lifetime (years, typically 0.267 yr)	$\tau_{\mathrm{O_3}}$

While we here focus on simple analytical metrics using simple parameterisations of the climate system, there is a variety of alternative approaches to develop emission metrics (Tanaka et al., 2010). One can conceptualise "climate models" as spanning from simple analytical models to complex general circulation models or earth-system models (IPCC, 2001; Held, 2005). Reisinger et al. (2010), Tanaka et al. (2009), and Azar and Johansson (2012) are examples of studies that use reduced complexity carbon cycle and energy balance models. In general, the more complex the models are, the better they represent the processes in the climate system, but at the cost of increasing computational time making them unsuitable for many common metric applications. Simple climate models with shorter computational times are used in some emission metrics (Tanaka et al., 2009; Wigley, 1998; Manne and Richels, 2001), but these are often difficult to represent in reduced analytical form. We focus in this article on analytical expressions to be able to provide a single consistent and transparent analytical framework that can handle a broad range of metric calculations. Despite the simplicity of these metrics, the key parameters are based on more complex climate models ensuring the metric values are realistic.

We now describe the key components of reduced form analytical emission metrics, and then develop the equations for common emission metrics. All the parameters used in the metrics are defined in Table 1. We develop the equations for emission pulses as this is most common for emission metrics,

since these can be used as building blocks for other applications. However, we later discuss the equations and results for sustained emissions and emission scenarios.

2.2 Impulse Response Function (IRF)

Once pollutants are emitted into the atmosphere, the pollutants will initially increase the atmospheric concentration before gradually being removed from the atmosphere leading to a decrease in concentration. In simple representations, the removal from the atmosphere for a pulse emission can be represented by a single or a sum of exponentials. Exponentials are particularly useful as they can be easily used in convolutions to represent the behaviour of arbitrary emissions scenarios (Enting, 2007), be converted into a set of differential equations for efficient solutions (Wigley, 1991), and in some cases the time scales in the IRF have physical interpretations (Li and Jarvis, 2009; Li et al., 2009). Most species can be represented by a single exponential (time-scale), though CO_2 is usually represented using multiple exponentials.

2.2.1 Multiple time-scales (CO_2)

For CO_2, the IRF is usually represented with multiple time scales (Archer et al., 2009), and it is assumed a fraction remains in the atmosphere indefinitely,

$$\mathrm{IRF}_{\mathrm{CO}_2}(t) = \sum_{i=0}^{I} a_i \exp\left(-\frac{t}{\tau_i}\right) \quad (2)$$

where $\Sigma a_i = 1$ and $\tau_0 = \infty$. Using this parameterisation, the decay of CO_2 does not reach zero at infinity, but converges to a non-zero value of a_0. The time scales in the decay parameterisation are not directly linked to any physical processes (Li et al., 2009); however, the time scales can be loosely interpreted as the uptake in land biosphere and the surface layer of the ocean for the short and decadal time scales, the surface layer mixing with the deep ocean for the century time scale, and the slow geological processes representing the millennia time scale (Archer and Brovkin, 2008; Archer et al., 2009). The literature suggests that "about 50 % of an increase in atmospheric CO_2 will be removed within 30 yr, a further 30 % will be removed within a few centuries and the remaining 20 % may remain in the atmosphere for many thousands of years" (Archer et al., 2009; IPCC, 2007). As the climate changes, the IRF will also change, as land and ocean may take up less CO_2 in a warmer climate (Friedlingstein et al., 2006).

The IRF for CO_2 that is used in emission metrics in the literature is usually based on the Bern carbon cycle model (Joos et al., 2001, 1996) with the IRF experimental setup described by Enting et al. (1994), also see Fig. 1 in Joos et al. (2013). Other studies have used other models or a range of carbon cycle models (e.g., Reisinger et al., 2010; Gillett and Matthews, 2010; Joos et al., 2013). The IRF is usually estimated in a two-step process (Enting et al., 1994; Joos et al., 2013), a control and perturbation run. First, for the control, the carbon cycle model is run with historical emissions until time t, and from t the emissions are calculated to keep a constant CO_2 concentration. Second, in the perturbation run, the emissions from the control are used, but a pulse emission is placed in $t+5$ and the model is allowed to run until near equilibrium. The pulse size is meant to be marginal (e.g., 1 kg CO_2) according to most metric definitions, but larger pulses (e.g., 100 GtC) are often used to get a good signal-to-noise ratio (Joos et al., 2013). The IRF is based on the normalised version of the difference between the perturbation and control run, after which a sum of exponentials is fitted.

Uncertainties in the carbon cycle and choices in the experimental setup, can have a large effect on the IRF (Wuebbles et al., 1995; Enting et al., 1994; IPCC, 1994; Archer et al., 2009; Eby et al., 2009; Joos et al., 2013). Different carbon cycle models lead to large differences in the IRFs, with differences of around 0.2 in a_0 after 500 yr (IPCC, 1994, Fig. 5.4; Enting et al., 1994, Fig. 9.1; Archer et al., 2009; Joos et al., 2013). Carbon cycle feedbacks can also lead to a large spread in the response of the carbon cycle (Friedlingstein et al., 2006) and consequently metric values (Gillett and Matthews, 2010; Reisinger et al., 2010).

The Bern Carbon Cycle model was used for the IRF in the Second, Third, and Fourth IPCC Assessment Reports, and the use of one model may give biased results compared to a model ensemble (Joos et al., 2013). Figure 1 shows the IRFs from the first four IPCC assessment reports and from a recent model intercomparison. In SAR, TAR, and AR4, the Bern Carbon Cycle was used, though each time it was improved making it difficult to determine if variations are due to model differences or changes in the background concentration. Using an experimental set up with a constant or scenario background to calculate the IRF, can lead to a difference in the IRF of 20 % after 500 yr (IPCC, 1994, Fig. 5.5; Enting et al., 1994, Figs. 9.1 and 9.2; Joos et al., 2013). In addition, the IRF will change depending on time the pulse is released in the experimental set up (IPCC, 1994, Fig. 5.5). Different pulse sizes also lead to different IRFs (Archer et al., 2009), but for use in metrics these are normalised to 1 kg to represent a marginal perturbation (Joos et al., 2013). Thus, the background, and its evolution, is an important determinant in the calculation of the IRF. The IPCC assessment reports are based on a constant background on which to allow transparent comparisons (Enting et al., 1994; IPCC, 1994). A recent model intercomparison shows that the response of the Bern model is similar to the model mean (Joos et al., 2013), as was the case for an earlier version of the Bern model (Enting et al., 1994).

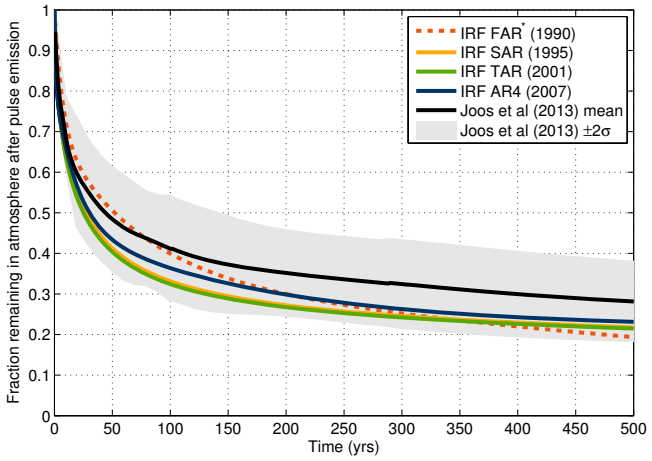

Fig. 1. The Impulse Response Function from the first four IPCC Assessment Reports. The values for the IRFs are from (IPCC, 1994) for FAR, IPCC (1995) for SAR, WMO (1999) for TAR which is the SAR IRF with a different parameterisation, IPCC (2007) for AR4, and Joos et al. (2013).The FAR IRF (dotted) is based on an unbalanced carbon-cycle model (ocean only) and, thus, is not directly comparable to the others. The SAR IRF is based the CO_2 response of the Bern model (Bern-SAR), an early generation reduced-form carbon cycle model (Joos et al., 1996), and uses a 10GtC pulse emission into a constant background without temperature feedbacks (Enting et al., 1994). The IRF was not updated for TAR, but a different parameterisation was used (WMO1999). The AR4 IRF is based on the Bern2.5CC Earth System Model of Intermediate Complexity (EMIC) (Plattner et al., 2008) and with a pulse size of 40 GtC and includes temperature feedbacks. The Joos et al. (2013) data is based on the model mean of a carbon cycle-climate model intercomparison project, which spans the full model hierarchy, and has specific pulse experiments. In each new IRF, the model has improved, so it is difficult to determine if the variations are due to improved scientific knowledge or changes in the background concentrations.

2.2.2 Single time-scales (non-CO_2 components)

Most species are assumed to follow a simple exponential decay with one time-scale:

$$\mathrm{IRF}_x(t) = \exp\left(-\frac{t}{\tau}\right) \tag{3}$$

Though, in practice, the decay may happen on different time scales for different processes and, thus, the atmospheric adjustment time may differ from the lifetime (Prather, 2007). Effects which change the adjustment time of a species are usually included among the "indirect effects" (e.g., Forster et al., 2007; Fuglestvedt et al., 1996). The time scale for chemically active species will, in general, vary as a function of time (e.g., Wigley et al., 2002; Voulgarakis et al., 2013), although these are modelled with constant adjustment time here. We mention several illustrative examples of species modelled with simple decay times here. N_2O removal in the atmosphere is mainly due to photolysis and reaction with metastable $O(^1D)$, both in the stratosphere leading to a time delay for transport to the stratosphere (Prather, 2007). Particles, such as black carbon, are removed by wet and dry deposition, hence, adjustment times are regionally dependent (Shindell and Faluvegi, 2009; Berntsen et al., 2006). CH_4 is removed from the atmosphere from three processes (Denman et al., 2007): (1) oxidation by hydroxyl radicals (OH) in the troposphere, (2) biological CH_4 oxidation in drier soil, and (3) loss to and destruction in the stratosphere. The first process enhances the methane's own lifetime through chemical coupling, thus, a feedback (by a factor of around 1.4 (Denman et al., 2007)), and these processes are nonlinear and dependent on the background concentrations of other species that interact with OH (Prather, 1994, 1996) causing its lifetime to be time-dependent in many applications (Wigley et al., 2002). The metric values we present for CH_4 are based on the adjustment lifetime of 12 yr, as given by Forster et al. (2007).

We have considered CH_4 as an independent species, but it is also possible to link CH_4 with the ozone precursors via a system of differential equations (c.f. Prather, 2007). Uncertainties in the lifetimes are due to uncertainties in the emission estimates and atmospheric chemistry (Prather et al., 2012).

2.2.3 Temperature

The temperature response to a given radiative forcing can be estimated using a range of complex or simple climate models. For emission metrics, a simplified IRF based on more complex models is usually used for the temperature response to an instantaneous unit pulse of RF, IRF_T (Shine et al., 2005b; Boucher and Reddy, 2008). Such an IRF does not take into account what species lead to the RF (see Sect. 4.2) or does not include any information on regional variations (see Sect. 4.1). A simple exponential parameterisation is usually used,

$$\mathrm{IRF}_T(t) = \sum_{j=1}^{J} \frac{c_j}{d_j} \exp\left(-\frac{t}{d_j}\right) \tag{4}$$

where the c_j add to give the climate sensitivity and d_j are the corresponding time scales. IRF_T can be mapped to a simple box-diffusion energy balance model, which aids in its interpretation (Peters et al., 2011a; Li and Jarvis, 2009; Berntsen and Fuglestvedt, 2008). The exponential term with the shortest time scale maps to the mixed atmosphere-ocean layer, the next largest time scale maps to the next deepest ocean layer and so on. The climate sensitivity can be determined by estimating the equilibrium response to a step (sustained) RF,

$$\lambda = \int_0^\infty \mathrm{IRF}_T(t)\,\mathrm{d}t = \sum_{j=1}^{J} c_j \tag{5}$$

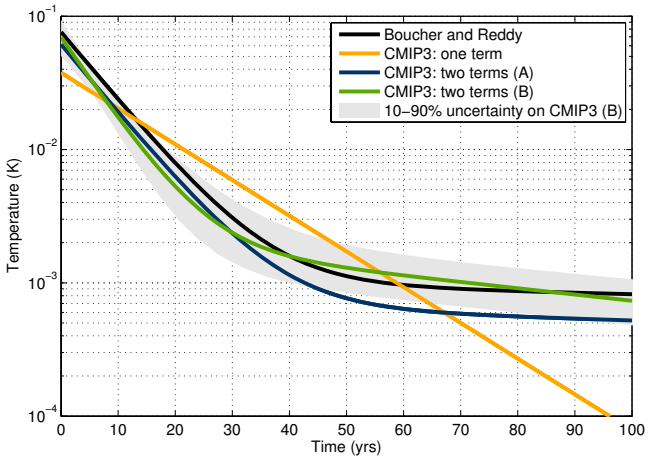

Fig. 2. The temperature response to a unit RF (log scale in temperature) from the Hadley model (Boucher and Reddy, 2008), and the CMIP3 ensemble mean with one exponential term and two exponential terms with different a priori values (Olivié et al., 2012). The IRF A uses an a priori estimate of 10 and 400 yr, while the IRF B uses an a priori estimate of 10 and 100 yr.

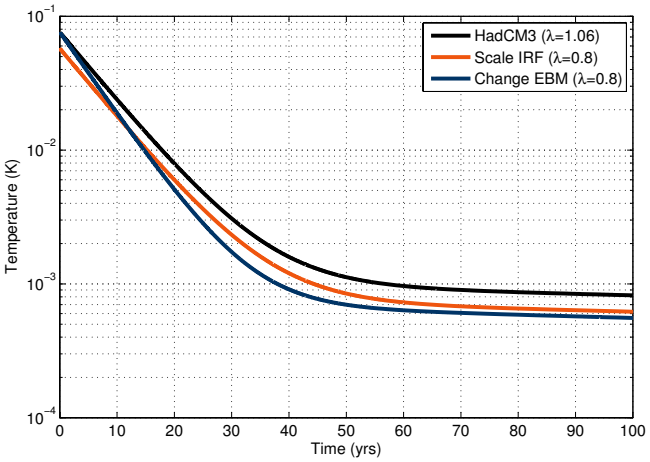

Fig. 3. The IRF from the Hadley model (Boucher and Reddy, 2008) compared to the Hadley IRF ($\lambda = 1.06$) scaled to $\lambda = 0.8$ and with the λ changed in a two-layer energy balance model (EBM) leading to different time constants.

The time scale to converge to the climate sensitivity is given by the largest d_i, and this can be more than several hundred years (Olivié et al., 2012). Since the time horizon is often less than the longest time scale, the climate sensitivity is not necessarily the most important parameter for emission metrics. Rather, the combination of c_j and d_j, particularly for the shorter time scales, are most relevant for the temperature response.

The parameters for IRF_T are usually calculated as a response in the global temperature to a pulse of RF, or experiments that allow a pulse to be estimated such as the C3MIP and C5MIP 1 % increasing CO_2 emission scenarios (Olivié et al., 2012). Most temperature based emission metrics use an IRF based on the Hadley model (Boucher and Reddy, 2008) response derived from more than 1000 yr of an experiment in which atmospheric CO_2 concentrations were quickly ramped up to 4 times the pre-industrial levels before being held constant. The parameters are derived from a curve fit to the response.

Olivié et al. (2012) estimated IRF_T for a range of models from the CMIP3 collection, Fig. 2, which indicates the model spread and dependence on experimental set up. Using a single exponential term does not give a realistic response compared to using 2 or 3 exponential terms, a similar conclusion was found by Li and Jarvis (2009). For the CMIP3 experiments, with relatively short integrations of 100–300 yr, two exponential terms are sufficient (Olivié et al., 2012), but for longer simulations three terms may be more representative (Li and Jarvis, 2009). The differences between the Hadley model and the CMIP3 ensemble, Fig. 2, represents both model variations and different integration lengths, with the Hadley model integrated to 1000 yr.

Until the work of Olivié et al. (2012); Olivié and Peters (2012), there has been relatively few IRF_T's available for different models. It is possible to modify the IRF_T of one model to match some aspects of another model, for example, the climate sensitivity. If the time constants of the IRF_T are assumed to be fixed, then the climate sensitivity can be scaled to match another model using a uniform scaling (e.g., $\mathrm{IRF}_{T,\mathrm{new}} = \lambda_{\mathrm{new}} \times \mathrm{IRF}_T / \sum c$, see Eq. 4). However, a different climate model is likely to have different time scales (Olivié et al., 2012) making the IRF parameters dependent on each other (Li and Jarvis, 2009; Peters et al., 2011a; Berntsen and Fuglestvedt, 2008) and, hence, modifying the climate sensitivity could also modify the time scales. Figure 3 shows the result of a simply scaling of the Hadley IRF to have a climate sensitivity of 0.8, a process which simply shifts the IRF vertically. If a two-layer box-diffusion model (Peters et al., 2011a) is based on the parameters of the Hadley model (specific heat capacities and vertical diffusivity), but the climate sensitivity of 0.8, then the IRF is different (Fig. 3) and the time scales change from 8.4 to 7.0 yr and 409.5 to 369.0 yr. This process assumes the specific heat capacities and vertical diffusivity are the same for the given λ, which is unlikely to be true. Thus, a better approach is to estimate an IRF for the specific climate model (Olivié et al., 2012). The applications presented in this paper use the IRF from Boucher and Reddy (2008).

2.3 Radiative efficiencies

Once a species is in the atmosphere and contributes to an increase in the atmospheric concentration of that component, it causes a radiative imbalance of energy in the earth system. The RF is usually calculated by complex radiative transfer models (Forster et al., 2007), but for emission

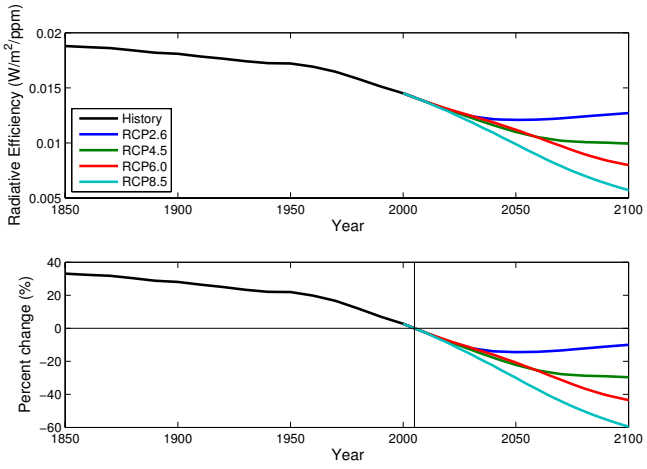

Fig. 4. The radiative efficiency (RE) for CO_2 as a function of concentration for the historic period and the Representative Concentration Pathways (RCPs) to be used in the IPCC Fifth Assessment Report. Constant current (2005) concentrations are represented by the 0 % line.

metrics simplifications are usually made, often based on the current state of the atmosphere. The RF is defined as the change in net irradiance at the tropopause after allowing for stratospheric temperatures to readjust to radiative equilibrium, while surface and tropospheric temperatures and state are held fixed at the unperturbed values (Ramaswamy et al., 2001; Hansen et al., 2005). The Radiative Efficiency (RE) is a linearisation of the modelled RF and is defined as the RF due to a unit increase in the concentration of a trace gas (IPCC, 1990).

In many papers, the RE is given with the unit $\mathrm{W\,m^{-2}\,ppb^{-1}}$, while the calculations in this paper is based on $\mathrm{W\,m^{-2}\,kg^{-1}}$. The conversion factor from ppb to kg is

$$C_X\,(\mathrm{kg}) = \left(\frac{M_\mathrm{A}}{M_X}\right) \times \left(\frac{10^9}{T_M}\right) \times C_X\,(\mathrm{ppb}) \tag{6}$$

where M_A is the mean molecular weight of air ($28.96\,\mathrm{kg\,mol^{-1}}$), M_X molecular weight of molecule X, and T_M total mass of the atmosphere (5.15×10^{18} kg) (Shine et al., 2005b). Recently, Prather et al. (2012) argued – after adjusting for water vapour in the atmosphere and transport into the stratosphere – that T_M is overestimated by 1–2 %.

2.3.1 Carbon Dioxide (CO_2)

The RF for CO_2 can be approximated using the expression based on radiative transfer models (Myhre et al., 1998),

$$\mathrm{RF} = \alpha \ln\left(\frac{C_0 + \Delta C}{C_0}\right) \tag{7}$$

where C_0 is the unperturbed atmospheric concentration of CO_2, ΔC is a perturbation over C_0, and $\alpha = 5.35$ is a constant. Forster et al. (2007) assessed this equation to be accurate within 10 %. The RE can be transparently defined as the marginal change in the RF as a function of the concentration increase,

$$A_{\mathrm{CO_2,\,marginal}} = \left.\frac{\mathrm{d}\,(\mathrm{RF})}{\mathrm{d}(\Delta C)}\right|_{\Delta C=0} = \frac{\alpha}{C_0} \tag{8}$$

and this approach has been used in several studies (Caldeira and Kasting, 1993; Lelieveld and Crutzen, 1992). The IPCC Assessment Reports, however, have estimated the RE using a small perturbation (ΔC)

$$A_{\mathrm{CO_2,\,average}} = \alpha \ln\left(\frac{C_0 + \Delta C}{C_0}\right)/\Delta C \tag{9}$$

In the Fourth Assessment Report, ΔC is taken as 1 ppm (Forster et al., 2007), while in the Third Assessment Report it is taken as the magnitude of the CO_2 pulse (IPCC, 2001; WMO, 1999). For small perturbations, the difference between approaches is negligible in comparison to the uncertainty in RF (see Table 2). In the metric calculations presented here, we use the small perturbation approach with $\Delta C = 1$ ppm.

Table 2. The two methods of calculating radiation efficiency for CO_2 is compared for different steps. The standard step for CO_2 is 1 ppm. The unperturbed concentration here is 378 ppm, which was measured in 2005 (Forster et al., 2007). As ΔC increases, the error in the step method increases almost linearly.

ΔC step	% Δ from d(RF)/dC to Δc step method
100 ppm	−12
10 ppm	−1.3
1 ppm	−0.13
1 ppb	−1.3e–4
1 ppt	−3.1e–6

Since the background concentration is constantly changing, the RE is technically a function of time (Fig. 4). As C_0 increases, the RE decreases and, hence, additional CO_2 becomes relatively less important. Compared to pre-industrial times, the RE in 2005 is 40 % lower and may be 50–100 % lower in 2100 depending on the future scenario (Fig. 4). Even if emission metrics are based on a constant background concentration, the background is usually different when metric values are updated (Reisinger et al., 2011) leading to a different RE. For a scenario background, the RE will change as a function of time within the metric calculation. In both constant and scenario backgrounds, the changes in concentration and hence RE are partially offset by changes in the IRF as a function of concentration (Caldeira and Kasting, 1993; Reisinger et al., 2011). For impact assessment, it can be argued to base the RE on a pre-determined fixed concentration such as pre-industrial concentrations (e.g., Huijbregts et al.,

2011). This would ensure that the metric values only change due to updated scientific information, but would mean that the relative weights of GHGs are based on pre-industrial conditions.

2.3.2 Methane (CH_4), Nitrous Oxide (N_2O), and other LLGHGs

As for CO_2, the RF estimates of CH_4 and N_2O are based on radiative transfer models (IPCC, 2001; Myhre et al., 1998):

$$\mathrm{RF}_{\mathrm{CH_4}=}\alpha_{\mathrm{CH_4}}\left(\sqrt{M}-\sqrt{M_0}\right)-[f(M,N_0)-f(M_0,N_0)] \quad (10)$$

and

$$\mathrm{RF}_{\mathrm{N_2O}=}\alpha_{\mathrm{N_2O}}\left(\sqrt{N}-\sqrt{N_0}\right)-[f(M_0,N)-f(M_0,N)] \quad (11)$$

where $\alpha_{\mathrm{CH_4}}=0.036$ and $\alpha_{\mathrm{N_2O}}=0.12$, M is the CH_4 concentration in ppb and N is the N_2O concentration in ppb, and the subscript 0 denotes the unperturbed concentration. The function f is

$$f(M,N)=0.47\ln\Big[1+2.01\times10^{-5}(MN)^{0.75} +5.31\times10^{-15}M(MN)^{1.52}\Big] \quad (12)$$

Further, the specific forcing of CH_4 is increased by a factor 1.4, due to effects on tropospheric ozone and stratospheric water vapour (IPCC, 2001; Forster et al., 2007). The RE is estimated using these equations, and as for CO_2, it is possible to estimate the RE using a marginal approach or the change due to a small perturbation.

The RE for other LLGHGs with low atmospheric concentrations, such as hydrochlorofluorocarbons (HCFCs) and hydrofluorocarbons (HFCs), can be estimated directly from their infrared absorption spectra of those species (Pinnock et al., 1995; Hodnebrog et al., 2013) and have constant RE with changing atmospheric concentrations. The uncertainty in the RE estimates for the LLGHGs is about 10 % (Forster et al., 2007).

2.3.3 Short-Lived Climate Forcers (SLCFs)

The RE for short-lived components is based on chemical transport models and RF calculations using Radiative Transfer Models (RTM) (Myhre et al., 2009; Skeie et al., 2011). The common approach to calculate the RE is to run a model perturbation which reduces the emissions by a certain fraction for one species at a time and then calculates the difference in radiative balance between this perturbed case and the reference simulation (Fuglestvedt et al., 2008; Forster et al., 2007). The RE is, then, calculated as the ratio between the calculated RF and change in burden. When we assume global average RF values for the SLCFs, even though there may be large regional variations, this simplification will lead to different REs and lifetimes (see Sect. 4.1). For some SLCFs, there are some non-standard issues in calculating the RE and the main ones are now explored.

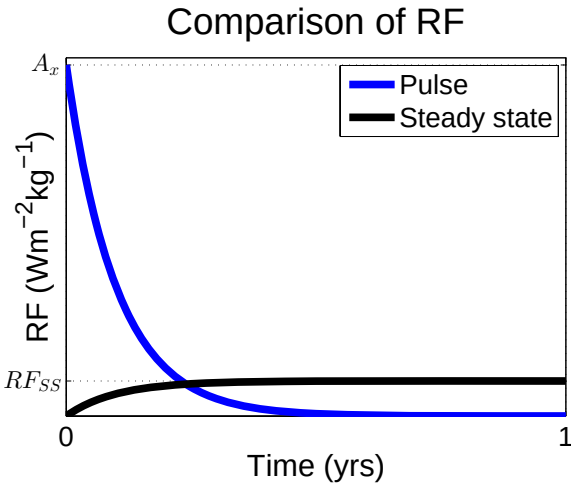

Fig. 5. For SLCFs with adjustment times much less than a year, the RF is usually calculated based on a sustained emission, $\mathrm{RF_{SS}}$, and then remapped back to the radiative efficiency, A_x.

Estimating RE for SLCF with adjustment times significantly less than one year

When the lifetime of the SLCF is significantly less than one year (e.g., a week or less), then some authors calculate the radiative efficiency (e.g., A_x) in two steps: first, calculate the RF after one year of constant steady-state emissions ($\mathrm{RF_{ss}}$), and second, by converting this to the radiative efficiency (e.g., A_x) for a pulse emission (Fuglestvedt et al., 2008). The main reason for using this method is that it provides an annual averaged value, avoiding variations in when the emissions occur. Figure 5 shows how $\mathrm{RF_{ss}}$ and A_x (defined in Table 1) compare for an arbitrary SLCF. Since the RF at time t for a sustained emissions is equivalent to the integrated RF up to time t of a pulse emissions (see Sect. 5.1), we can estimate the correct RE, A_x, as

$$\mathrm{RF_{ss}}(H=1)=\int_0^1 A_x e^{-\frac{t}{\tau}}=-\tau A_x\left(e^{-\frac{1}{\tau}}-1\right)\approx\tau A_x \quad (13)$$

where we assumed $\exp(-1/\tau)$ is negligible since $\tau\ll1$, hence,

$$A_x\approx\frac{\mathrm{RF_{ss}}}{\tau} \quad (14)$$

2.4 Inclusion of indirect effects

2.4.1 Chemical reactions

Emissions of chemically active species can have both direct and indirect effects on radiative forcing. Indirect effects are a consequence of chemical reactions which lead to changes in concentrations of other species which have radiative effects. The most relevant indirect effects are emissions linked

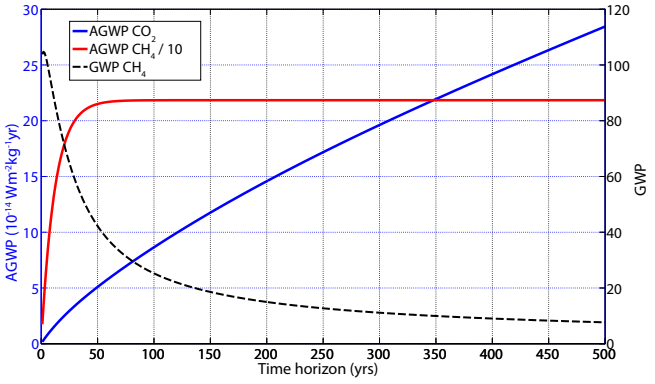

Fig. 6. The GWP_{CH_4} as a function of time, showing how it is affected by AGWP for both CH_4 and CO_2 with changing time horizons.

to tropospheric ozone formation or destruction, enhancement of stratospheric water vapour, changes in concentrations of the OH radical (which controls the lifetime of several radiatively active species; e.g., CH_4, HCFCs), and secondary aerosol formation. CH_4, as discussed earlier, has both direct effects due to CH_4 itself and indirect effects due to chemical reactions which increase the lifetime of CH_4 and lead to O_3 production (Forster et al., 2007; Fuglestvedt et al., 2010). Recently, it has been suggested that the oxidation of fossil fuel based CH_4 to CO_2 should be included as an indirect effect (Boucher et al., 2009) and even the carbon cycle feedbacks on CO_2 (Collins et al., 2013). Emissions of VOC, NO_x, and CO have no direct radiative effects, but through chemical reactions lead to O_3 production and changes in OH, and hence radiative effects. Shindell et al. (2009) further find that including interactions with aerosols increases the best estimate of the GWP100 value for CH_4 and CO and decreases the value for NO_x. Some species have only indirect effects (for example, VOC, NO_x, and CO), while others are dominated by direct effects. Given the complexity of interactions, choices are required to decide which interactions are included as indirect effects. The metric values we present for CH_4 includes the direct effect of CH_4 and the indirect effect via OH by using the adjustment time instead of the lifetime. Further, by adjusting the RE to account for the indirect effects on tropospheric ozone and stratospheric water vapour, these two indirect effects are also included. For NO_x, CO, and VOC, we include the indirect short-lived O_3 effect, CH_4 effect, and CH_4-induced O_3 effect. We do not include the oxidation of CH_4 to CO_2.

2.4.2 Black Carbon on snow and ice

For BC, there is an indirect effect of BC deposited on snow and ice as BC reduces the albedo of such surfaces (Warren and Wiscombe, 1980; Jacobson, 2001; Hansen and Nazarenko, 2004; Rypdal et al., 2009; Doherty et al., 2010). The indirect effect of BC on snow and ice raises the impact by 10–15 % depending on the location of emissions (Rypdal et al., 2009; Bond et al., 2011).

2.4.3 Ozone depleting substances (ODS)

Chlorine- and bromine-containing halocarbons cause ozone depletion in the stratosphere. While the direct effect of the ODS is warming, they also have a cooling effect via reduction of stratospheric ozone, which may be included in metrics (Daniel et al., 1995).

2.4.4 Contrails and cirrus

Aviation also leads to indirect impacts on climate through formation of contrails and aviation induced cirrus (AIC) due to the high-altitude emission of water vapour and particles. These indirect effects are large, but also have large uncertainties, and their impact will vary greatly due to different flight paths (both horizontally and vertically). The uncertainty on the RF of contrails is in the order of 1.5 to 2 and for AIC about an order of 3 (Fuglestvedt et al., 2010). Anthropogenic aerosols will also influence upper tropospheric clouds through ice nucleation (Penner et al., 2009; Liu et al., 2009; Hendricks et al., 2011).

2.4.5 Aerosol Indirect Effect (AIE)

Aerosols have both direct and indirect effects on RF. The direct effects are due to scattering and absorption of radiation, while the indirect effects modify the microphysical and, hence, the radiative properties, amount and lifetime of clouds. The semi-direct effect includes heating from the aerosols, which result in a cloud burn-off. Aerosols will also impact mix-phase and ice clouds, but the RF from that effect is uncertain (Lohmann and Feichter, 2005). The AIE have usually been split into “cloud albedo effect” (first indirect effect) and the “cloud lifetime effect” (second indirect effect) (Forster et al., 2007). It is difficult to separate which aerosols contribute to the AIE. The central estimate in Forster et al. (2007) indicates that the indirect effect is roughly 40 % larger than the direct effect, with a factor of 1.5–2 to account for AIE relative to just the direct effect of sulfate aerosols (though uncertainty is large).

3 Metric equations

3.1 Absolute metrics

In the following sections, we present analytical expressions for the different metrics. Emission metrics are obtained by combining the information on the radiative efficiency with IRFs, and, thus, emission metrics only approximate the response of more complex models. However, on the assumption that the emission metrics are applied to marginal emission changes and the metrics are applied to background

conditions consistent with the derivation of the metric parameters, these responses should agree to within first-order of the actual response. The largest differences are expected for short-lived species where the location and timing of emissions are important (Lund et al., 2011).

3.1.1 Radiative forcing (RF) as function of t

For emission metrics, the radiative forcing (RF) for all components is calculated as

$$\mathrm{RF} = \mathrm{RE} \times \mathrm{IRF}. \tag{15}$$

In the context of Eq. (1), the impact is RF, and the discount is a Dirac delta function at time t leading to an end-point metric. Based on the equations above, the RF for CO_2 is

$$\mathrm{RF}_{\mathrm{CO_2}}(t) = A_{\mathrm{CO_2}} \left\{ a_0 + \sum_{i=1}^{\mathrm{I}} a_{\mathrm{i}} \left(1 - \exp\left(-\frac{t}{\tau_{\mathrm{i}}} \right) \right) \right\} \tag{16}$$

Further, the equivalent expression for pollutants with a simple exponential decay is

$$\mathrm{RF}_{\mathrm{x}}(t) = A_{\mathrm{x}} \exp\left[-\frac{t}{\tau} \right] \tag{17}$$

The RF for the ozone precursors (OP: NO_x, CO, VOC considered here) is, however, more complex. Due to their short lifetime, it is assumed that the pulse emission lasts one year with constant emissions through the year followed by decay in concentration after end of year 1 (see Sect. 2.3.3) (Fuglestvedt et al., 2010). Hence, the parameterisation of RF is split into two parts, the RF that is due the first year of emissions ($t < 1$) and the RF due to the decaying concentration afterwards. The OPs have an insignificant direct effect on RF; however, there are three indirect effects due to chemical reactions. The short-lived O_3 effect occurs for all the species as a positive RF due to the formation of tropospheric O_3. CO and VOC (NO_x) cause a positive (negative) RF by decreasing (increasing) the OH levels and, thus, increasing (decreasing) the CH_4 levels, which is the CH_4 effect. Since the CH_4 concentration is perturbed, a secondary effect impacts the O_3, called the CH_4-induced O_3 effect. Hence, CO and VOC (NO_x) will have a positive (negative) RF due to increased (decreased) O_3 caused by the CH_4 perturbation. The perturbations for each of the three effects are

$$\mathrm{RF}^{S}_{\mathrm{OP}}(t) = \begin{cases} A^{S}_{\mathrm{OP}} \left(1 - \exp\left(-\frac{t}{\tau} \right) \right) & 0 < t < 1 \\ A^{S}_{\mathrm{OP}} \left(1 - \exp\left(-\frac{1}{\tau} \right) \right) \exp\left(-\frac{t-1}{\tau} \right) & t \geq 1 \end{cases} \tag{18}$$

where OP is the ozone precursors and S is one of the three perturbation effects: (1) short-lived O_3 effect, (2) CH_4 effect, and (3) CH_4-induced O_3 effect. The lifetime τ is τ_{O_3} for the short-lived O_3 perturbation and τ_{PM} for the CH_4 perturbation and CH_4-induced O_3 perturbation. τ_{PM} is the primary mode methane adjustment time. This formulation differs slightly from Fuglestvedt et al. (2010), as they assumed that the very small contribution from the CH_4-induced O_3 perturbation in year 1 to be included in the short-lived O_3 response, whereas we do not make this assumption. The final RF from the three effects is

$$\mathrm{RF}_{\mathrm{OP}}(t) = \sum_{s=1}^{S} \mathrm{RF}^{S}_{\mathrm{OP}} \tag{19}$$

where OP is either NO_x, CO, or VOC.

3.1.2 Absolute Global Warming Potential (AGWP)

The absolute Global Warming Potential (AGWP) for species i is the integrated RF,

$$\mathrm{AGWP}_i(H) = \int_0^H \mathrm{RF}_i(t)\,\mathrm{d}t \tag{20}$$

In the context of Eq. (1), the impact is RF, with the discounting as a step function (no discounting for $t < H$ and full discounting for $t > H$). Fuglestvedt et al. (2003) estimated an equivalent exponential discount function that gave the same AGWP and found that different species implicitly had different discount rates. The IPCC did not give a direct physical interpretation of the AGWP, but gave some tentative interpretations for three time horizons (20, 100, 500 yr) (IPCC, 1990). They describe that for some environmental impacts it is important to evaluate the cumulative warming over an extended period after the emissions. For instance, the evaluation of sea level rise needs a time horizon of 100 yr or longer. For short term effects, a time horizon of a few decades could be used, such as the response to RF over continental areas.

The AGWP for CO_2 is

$$\mathrm{AGWP}_{\mathrm{CO_2}}(H) = A_{\mathrm{CO_2}} \left\{ a_0 H + \sum_{i=1}^{\mathrm{I}} a_{\mathrm{i}} \tau_{\mathrm{i}} \left(1 - \exp\left(-\frac{H}{\tau_{\mathrm{i}}} \right) \right) \right\} \tag{21}$$

and for pollutants with a simple exponential decay

$$\mathrm{AGWP}_x(H) = A_x \tau \left(1 - \exp\left(-\frac{H}{\tau} \right) \right) \tag{22}$$

The formulas are more complex for the ozone precursors (NO_x, CO, VOC), since they have a short-lived O_3 effect, CH_4 effect, and CH_4-induced O_3 effect. Those effects are parameterised as

$$\mathrm{AGWP}^{S}_{\mathrm{OP}}(t) = \begin{cases} A^{S}_{\mathrm{OP}} \left\{ H - \tau \left[1 - \exp\left(-\frac{H}{\tau} \right) \right] \right\} & 0 < t < 1 \\ A^{S}_{\mathrm{OP}} \left\{ 1 - \tau \left[\exp\left(-\frac{(H-1)}{\tau} \right) - \exp\left(-\frac{H}{\tau} \right) \right] \right\} & t \geq 1 \end{cases} \tag{23}$$

with different RE A^S_{OP} and lifetime τ for the different perturbations, see Eq. (18). The total effect of the ozone precursor is

$$\mathrm{AGWP}_{\mathrm{OP}}(t) = \sum_{s=1}^{S} \mathrm{AGWP}^S_{\mathrm{OP}} \tag{24}$$

3.1.3 Absolute Global Temperature change Potential (AGTP)

The absolute Global Temperature change Potential (AGTP) for species i is the global temperature change (ΔT) at time t (Shine et al., 2005b),

$$\mathrm{AGTP}_i(H) = \int_0^t \mathrm{RF}_i(t)\,\mathrm{IRF}_T(H-t)\,\mathrm{d}t, \tag{25}$$

In terms of Eq. (1), the impact is temperature (the whole integral) with a Dirac delta function used for discounting (an end-point indicator) with an evaluation time of t. The expression for AGTP also helps to interpret the AGWP. If it is assumed (unrealistically) that $\mathrm{IRF}_T = 1$, then the AGTP equation simplifies to the AGWP. Thus, the AGWP integrates ("remembers") the RF for all times up to H. If it is assumed (realistically) that $\mathrm{IRF}_T \neq 1$ and is a monotonically decreasing function, then IRF_T can be interpreted as a physical discounting (as energy radiated back to space is modulated by the thermal inertia and mixing in the ocean). Using these analogies for IRF_T helps explain why SLCFs generally have higher GWP values compared to GTP values; the GWP integrates all the RF in a given time period, while the GTP allows a physical discounting (via ocean inertia), so that RF values at earlier time periods receive less weight (see Peters et al., 2011a).

The AGTP for CO_2 is

$$\mathrm{AGTP}_{\mathrm{CO_2}}(H) = A_{\mathrm{CO_2}} \left\{ \sum_{j=1}^{J} a_0 c_j \left[1 - \exp\left(-\frac{H}{d_j}\right)\right] + \sum_{i=1}^{I}\sum_{j=1}^{J} \frac{a_i \tau_i c_j}{\tau_i - d_j} \left[\exp\left(-\frac{H}{\tau_i}\right) - \exp\left(-\frac{H}{d_j}\right)\right]\right\} \tag{26}$$

For pollutants with a simple exponential decay

$$\mathrm{AGTP}_x(H) = \sum_{j=1}^{J} \frac{A_x \tau c_j}{(\tau - d_j)} \left[\exp\left(-\frac{H}{\tau}\right) - \exp\left(-\frac{H}{d_j}\right)\right] \tag{27}$$

The formulas are more complex for the ozone precursors (NO_x, CO, VOC), since they have a short-lived O_3 effect, CH_4 effect, and CH_4-induced O_3 effect. For all these effects, there is a perturbation from the RF for $t < 1$ (this determines the temperature response of the emissions that occur in the first year) and from the RF for $t \geq 1$ (this determines the temperature response of atmospheric perturbation lasting past one year). Thus, $\mathrm{AGTP}_{\mathrm{OP}}$ for $H > 1$ is comprised of two components ($\mathrm{AGTP}(H) = \mathrm{AGTP}^{S,<1}_{\mathrm{OP}}(\mathrm{H}) + \mathrm{AGTP}^{S,>1}_{\mathrm{OP}}(H)$):

a. For perturbation from RF occurring $t < 1$

$$\mathrm{AGTP}^{S,<1}_{\mathrm{OP}}(H) = A^S_{\mathrm{OP}} \sum_{j=1}^{J} \left\{ c_j \left[\exp\left(\frac{1-H}{d_j}\right) - \exp\left(-\frac{H}{d_j}\right)\right] + \frac{c_j \tau}{\tau - d_j} \left[\exp\left(-\frac{H}{d_j}\right) - \exp\left(\frac{1-H}{d_j}\right)\exp\left(-\frac{1}{\tau}\right)\right]\right\} \tag{28}$$

b. For perturbation from RF occurring $t \geq 1$

$$\mathrm{AGTP}^{S,>1}_{\mathrm{OP}}(H) = A^S_{\mathrm{OP}} \left[1 - \exp\left(-\frac{1}{\tau}\right)\right] \sum_{j=1}^{J} \frac{\tau c_j}{\tau - d_j} \left[\exp\left(\frac{1-H}{\tau}\right) - \exp\left(\frac{1-H}{d_j}\right)\right] \tag{29}$$

The RE A^S_{OP} and lifetime τ differ between the different perturbations, see Eq. (18). These formulas are only valid when $H > 1$, and for continuity it is possible to make a linear interpolation ($aH + b$) between year 0 (where the perturbation is $\mathrm{AGTP}^S_{\mathrm{OP}}(0) = 0$) and year 1. This step is not necessary based on physical processes, but is done to ensure continuity in graphical presentation and for calculating the integrated AGTP (next section). For all the three different ozone precursor perturbations, the perturbation for $0 < H < 1$ is given by

$$\mathrm{AGTP}^S_{\mathrm{OP}}(H) = \mathrm{AGTP}^S_{\mathrm{OP}}(1)\,H, \quad \text{for} \quad 0<H<1 \tag{30}$$

It is possible to extend the AGTP into a regional form (c.f. Shindell, 2012),

$$\mathrm{ARTP}^{\mathrm{r}}_i(H) = \int_0^t \sum\nolimits_{\mathrm{s}} \left(K^{\mathrm{rs}}_i \mathrm{RF}^{\mathrm{s}}_i\right) \mathrm{IRF}_T(H-t)\,\mathrm{d}t, \tag{31}$$

where "r" represents the region with the response, "s" the region of the RF, and K^{rs} a matrix of scalars relating the RF in "s" to the response in "r", see Fig. 7. A similar expression is possible to link regional emissions with RF and, hence, from regional emissions to regional responses.

3.1.4 Integrated Absolute Global Temperature change Potential (iAGTP)

The integrated absolute Global Temperature change Potential (iAGTP) for species i is the integral of the AGTP_i (Peters et al., 2011a; Azar and Johansson, 2012),

$$\mathrm{iAGTP}_i(H) = \int_0^t \mathrm{AGTP}_i(t)\,\mathrm{d}t \tag{32}$$

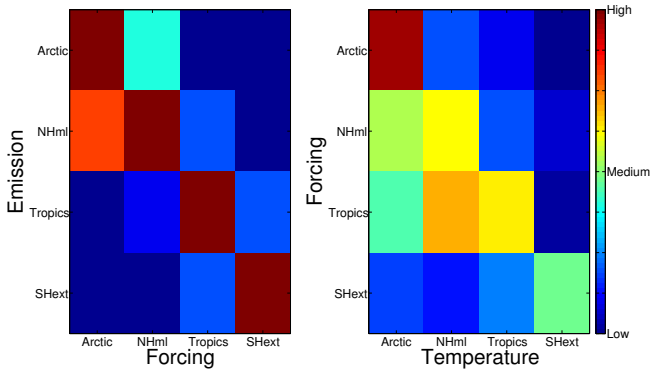

Fig. 7. A schematic regional relationship between emission, RF, and temperature perturbation for SLCFs for the regions: The Southern Hemisphere extratropics (90–28° S, SHext), the tropics (28° S–28° N), the Northern Hemisphere mid-latitudes (28–60° N, NHml), and the Arctic (60–90° N). Values for the emission-RF relationship is inspired by Naik et al. (2005) and the RF-temperature relationship is based on Shindell (2012).

Similar metrics have been proposed before. Gillett and Matthews (2010) introduced the Mean Global Temperature Potential, MGTP(H) = iAGTP(H)/H. Jacobson (2010) introduced the "surface temperature response per unit continuous emissions" (STRE), which is mathematically equivalent to the iAGTP, though Jacobson (2010) uses a single decay for CO_2, which is different from what is done in the other studies and by IPCC (Forster et al., 2007; Archer et al., 2009; Joos et al., 2013).

In terms of Eq. (1), the impact is temperature, and the discount function is no discounting for $t < H$ and full discounting for $t > H$. The iAGTP has been discussed indirectly by some authors (O'Neill, 2000; Gillett and Matthews, 2010), but in more detail in Peters et al. (2011a); Azar and Johansson (2012). Preliminary work on the GWP was also based on integrated temperature change (Wuebbles, 1989; Derwent et al., 1990), but the link to temperature did not make it into the First Assessment Report (IPCC, 1990). Peters et al. (2011a); Azar and Johansson (2012) investigated whether the GWP was similar to the iGTP and found close agreement for a wide range of time horizons, but not for very SLCFs like BC. The similarity is since AGWP represents the total energy added to the system and iAGTP/λ the energy lost from the system. Since the energy currently in the system is small relative to AGWP, it follows that AGWP is approximately iAGTP/λ. Given these quantitative relationships, it can be argued to interpret the AGWP as iAGTP.

The iAGTP for CO_2 is (Peters et al., 2011a)

$$\text{iAGTP}_{CO_2} = A_{CO_2}\left\{\sum_{j=1}^{J} a_0 c_j\left[H - d_j\left(1-\exp\left(-\frac{H}{d_j}\right)\right)\right]\right.$$
$$+\sum_{i=1}^{I}\sum_{j=1}^{J}\frac{a_i\tau_i c_j}{\tau_i - d_j}\left[\tau_i\left(1-\exp\left(-\frac{H}{\tau_i}\right)\right)\right.$$
$$\left.\left.-d_j\left(1-\exp\left(-\frac{H}{d_j}\right)\right)\right]\right\} \quad (33)$$

While the iAGTP for species with a single decay time is

$$\text{iAGTP}_x(H) = \sum_{j=1}^{J}\frac{A_x\tau c_j}{(\tau - d_j)}\left[\tau\left(1-\exp\left(-\frac{H}{\tau}\right)\right)\right.$$
$$\left.-d_j\left(1-\exp\left(-\frac{H}{d_j}\right)\right)\right] \quad (34)$$

For the ozone precursor perturbations, the linear interpolation between year 0 and year 1 for AGTP turns into a quadratic form $(\frac{a}{2}H + bH^2)$ for the iAGTP. In the range $0 < H < 1$, the perturbation is

$$\text{iAGTP}^S_{\text{OP}}(H) = \frac{1}{2}\text{AGTP}^S_{\text{OP}}(1)\,H^2 \quad (35)$$

This formula is used when $H \leq 1$. For all other times, $\text{iAGTP}^S_{\text{OP}}(1)$ has to be added into the formula. For $H > 1$, $\text{iAGTP}^S_{\text{OP}}$ has to be summed for the RF from $t < 1$ and for the RF from $t > 1$. Thus, $\text{iAGTP}^S_{\text{OP}}$ for $H > 1$ is comprised of two components ($\text{iAGTP}(H) = \text{iAGTP}^{S,<1}_{\text{OP}}(H) + \text{iAGTP}^{S,>1}_{\text{OP}}(H)$):

a. For perturbation from RF occurring $H < 1$

$$\text{iAGTP}^{S,<1}_{\text{OP}}(H) =$$
$$\text{iAGTP}^S_{\text{OP}}(1) + A^S_{\text{OP}}\sum_{j=1}^{J}\left\{c_j d_j\left[1-\exp\right.\right.$$
$$\left(\frac{1-H}{d_j}\right)+\exp\left(-\frac{H}{d_j}\right)-\exp\left(-\frac{1}{d_j}+\frac{c_j d_j\tau}{\tau-d_j}\right)\Big]$$
$$\left[\exp\left(-\frac{1}{d_j}\right)-\exp\left(-\frac{H}{d_j}\right)-\left(1-\exp\left(\frac{1-H}{d_j}\right)\right)\right.$$
$$\left.\left.\exp\left(-\frac{1}{\tau}\right)\right]\right\} \quad (36)$$

b. For perturbation from RF occurring $H \geq 1$

$$\text{iAGTP}^{S,>1}_{\text{OP}}(H) =$$
$$\text{iAGTP}^S_{\text{OP}}(1) + A^S_{\text{OP}}\left[1-\exp\left(-\frac{1}{\tau}\right)\right]$$
$$\sum_{j=1}^{J}\frac{\tau c_j}{\tau-d_j}\left[\tau\left(1-\exp\left(\frac{1-H}{\tau}\right)\right)\right.$$
$$\left.-d_j\left(1-\exp\left(\frac{1-H}{d_j}\right)\right)\right] \quad (37)$$

As previously, the RE A^S_{OP} and lifetime τ differ between the different perturbations, see Eq. (18).

3.2 Normalised metrics

The absolute metrics for a species are often normalised to the corresponding absolute metric for a reference gas, normally CO_2,

$$M_x(t) = \frac{\mathrm{AM}_x(t)}{\mathrm{AM}_{\mathrm{CO}_2}(t)} \tag{38}$$

where AM stands for AGWP, AGTP, or iAGTP and M is GWP, GTP, or iGTP, respectively. Emissions E_x are usually converted into "CO_2 equivalent emissions" by multiplying with this normalised metric,

$$\mathrm{CO_2eq}(t) = M_x(t) \times E_x \tag{39}$$

that would ideally result in the same climate response for the given metric. Thus, the normalised metric value can be considered as a conversion factor from the unit of the emission (e.g., kg CH_4) to the "equivalent" emission of CO_2 that would ideally lead to the equivalent climate impact for the given TH and underlying assumptions (Fuglestvedt et al., 2003; O'Neill, 2000). But this equivalence is not present for other climate variables beyond what the metric measures and how it measures it. The choice of reference gas is a value based choice, but an obvious choice is to use the trace gas of primary concern, namely carbon dioxide (IPCC, 1990). There is no natural need to have only one reference gas or let CO_2 always be the reference gas. A two-basket or multi-basket approach to climate policy could be used to treat species with different lifetimes differently, and each basket may have a different reference gas (e.g., Smith et al., 2012; Daniel et al., 2012).

The normalised metric is dependent on the absolute metric of CO_2, since the absolute metric of CO_2 is the denominator. In a multiple baskets approach, several different reference gases could be used. We show the importance of the denominator, here CO_2, in the case of CH_4 for GWP in Fig. 6. For time horizons (H) less or around a species' lifetime (τ), GWP is affected by AGWP for both the species and CO_2, as both AGWPs are sensitive of time horizon. However, as time horizon increases, the changes in the GWP depend only on the changes in AGWP for CO_2 since the AGWP for CH_4 converges to its steady-state value soon after the lifetime (dependent on the e-folding time). The same is true for all SLCFs, where species reach this threshold increasingly faster with decreasing lifetimes. Hence, for $\tau \ll H$, the changes in the GWP value of a species depends only on the behaviour of CO_2 (e.g., BC the order of months, or CH_4 the order of decades).

3.3 Metrics based on economic models

Some emission metrics have been based on economic models. Manne and Richels (2001) investigated how constraints will affect the "price ratio" of different LLGHGs and compared with the GWP. Recently, the Global Cost Potential (GCP) and Cost-Effective Temperature Potential (CETP) were developed (Johansson, 2012), which show similar characteristics to the Manne and Richels (2001) study. The time-dependent version of the GTP (Shine et al., 2007) puts more weight on SLCFs and shorter-lived LLGHGs as the target is approached, a characteristic seen in many economic approaches (Manne and Richels, 2001; Johansson, 2012). Since this property occurs in the purely physical based metric, it may suggest that this property is a result of moving towards a target and not a consequence of including an economic model in the metric. For a cost-benefit framework, the Global Damage Potential (GDP) is suitable, which looks at the marginal damages of emissions (Kandlikar, 1995; Boucher, 2012; Tol et al., 2012).

4 Cross-cutting issues

There are a variety of cross-cutting issues which affect most metrics in a similar way. For example, the RF can be allowed to vary by region leading to regional metric values. We discuss a variety of the most relevant cross-cutting issues here.

4.1 Regional metric values

While the location of emissions does not have an impact on the RF for LLGHGs, it does for SLCFs (Fuglestvedt et al., 1999; Naik et al., 2005; Berntsen et al., 2006; Shindell and Faluvegi, 2009) leading to a regional distribution of RF for a given emission (Berntsen et al., 2006; Bond et al., 2011). For all forcings, even the relatively homogeneous ones caused by LLGHGs, there is a distinct pattern in the temperature response controlled largely by the response pattern of the climate feedbacks (Boer and Yu, 2003; Shindell and Faluvegi, 2009; Shindell, 2012). Combing these two effects for a given emission of a SLCF, the heterogeneity in RF may cause further inhomogeneity in the climate response.

A schematic presentation of the regional effects is given in Fig. 7. Those SLCFs that have an atmospheric residence time of a couple of weeks or less will not have time to be evenly distributed in the global atmosphere and, hence, result in the largest concentration perturbations near the point of emission and its latitude band. In general, strong climate feedbacks at higher latitudes increase the temperature perturbations from RFs, with about 45 % enhancement for extra-tropical relative to tropical CO_2 RF (Shindell and Faluvegi, 2009). The enhanced regional sensitivities at higher latitudes are a result of higher sensitivity in the energy budget in those regions, which is governed by local cloud, water vapour and surface albedo feedbacks. Vertical profiles of radiative forcing efficiencies are also a source of regional differences. For example, black carbon, which is found low in the atmosphere near emission sources and higher up in transport regions, has

a steeply increasing forcing efficiency with altitude (Samset and Myhre, 2011). The relative position of BC to clouds is also important, as are seasonal changes in cloud fraction, insolation, wind and precipitation. Similar considerations exist for other SLCFs. In addition to variability in physical and chemical key parameters, there are strong nonlinear relations in the atmospheric chemistry (Shindell and Faluvegi, 2009).

While most parameterisations of impacts parameters are for global means, metric research has also focused on metrics accounting for regional variations (Shine et al., 2005a; Lund et al., 2011) or regional metrics (Berntsen et al., 2005; Fuglestvedt et al., 2010; Fry et al., 2012; Collins et al., 2013). Shindell and Faluvegi (2009) separate the world into four latitude bands and estimated regional responses from regional RFs for some selected LLGHGs and SLCFs, though it is feasible to do this at smaller scales (Henze et al., 2012). This work has been extended by introducing the Absolute Regional Temperature Potential (ARTP) (Shindell, 2012; Collins et al., 2013).

4.2 Efficacy

The temperature perturbation from the RF can also depend on the type of forcing agent, leading to the concept of efficacy, which is defined "as the ratio of the climate sensitivity parameter for a given RF agent (λ_i) to the climate sensitivity parameter for CO_2 changes, that is, $\varepsilon_i = \lambda_i/\lambda_{CO_2}$" (Forster et al., 2007). The efficacy moves one step closer to the actual temperature response by accounting for differences in how various components trigger feedbacks. Efficacies are usually between 0.75 and 1.25 for most components; however, for absorbing aerosols the range is larger and even the idea of an efficacy becomes complicated (Forster et al., 2007). Fuglestvedt et al. (2003) proposed and Berntsen et al. (2005); Berntsen and Fuglestvedt (2008) applied the efficacy concept to simple emission metrics.

4.3 Consistency across assumptions

Despite the wide-spread use of emission metrics, there has not been a systematic and fully consistent estimation of the numeric values of particular metrics. It is routine to combine different, and potentially inconsistent, models in a given metric; for example, it is common that the $AGTP_{CO_2}$ uses the Bern model for the carbon cycle and the Hadley model for the temperature response. There is no consistency on which feedbacks and indirect effects to include implying that the IRF for one species may include temperature feedbacks (e.g., CO_2) and another species may not (e.g., CH_4 and N_2O). Recent research has included additional indirect effects, such as those on aerosols (e.g., Shindell et al., 2009), effects of O_3 on vegetation (Collins et al., 2010), and temperature feedbacks (Gillett and Matthews, 2010; Collins et al., 2013). Different assumptions can also be used to estimate the parameters for metrics, such as different background concentrations and pulse sizes (Joos et al., 2013). It is not clear how large these consistency issues may be, nor how model dependent they may be.

Many of these consistency issues can be overcome by a clear set of definitions for each metric, particularly on how to treat indirect effects and feedbacks. One way of achieving more consistency is through model intercomparisons (e.g., Olivié and Peters, 2012; Joos et al., 2013). Through a model intercomparison, or the use of individual models (e.g., Reisinger et al., 2010; Gillett and Matthews, 2010), the same model can be used to estimate all metric values. Joos et al. (2013), for example, estimate the $AGWP_{CO_2}$ and $AGTP_{CO_2}$ directly from pulse emissions of CO_2 and, thus, ensuring consistency.

4.4 Relative uncertainty from parameters and choices

Several recent studies have investigated uncertainty in metric values (Reisinger et al., 2010; Boucher, 2012; Olivié and Peters, 2012). These approaches have been either based on model comparisons or Monte-Carlo approaches. The studies suggest that uncertainties are significantly larger than previously reported (e.g., Forster et al., 2007), the relative uncertainties for the GTP are larger than for the GWP, and revisions of the GWP and GTP values should be expected as scientific knowledge advances (e.g., Reisinger et al., 2011). Uncertainties in GWP_{CH_4} are generally found to be of the order of 40 % (for 5–95 % confidence interval) for a 100 yr time horizon.

It is possible to assess uncertainty more generally using standard methods of uncertainty propagation. For a general function, f, with two independent variables, x and y, the uncertainty in f can be approximated as

$$\Delta f = \sqrt{\left(\frac{\partial f}{\partial x}\right)^2 \Delta x^2 + \left(\frac{\partial f}{\partial y}\right)^2 \Delta y^2} \tag{40}$$

This allows the combination of different pieces of information on uncertainty (e.g., from independent studies) to assess the main causes of the uncertainty in emissions metrics (e.g., RE versus IRF). We demonstrate the use of this approach using CH_4 as an example. The uncertainty in each of the metric components propagates to the total uncertainty in the metric parameterisations. For instance, the uncertainty for AGWP is given by

$$\Delta \mathrm{AGWP} = \sqrt{\left(\frac{\partial \mathrm{AGWP}}{\partial A}\right)^2 \Delta A^2 + \left(\frac{\partial \mathrm{AGWP}}{\partial \tau}\right)^2 \Delta \tau^2} \tag{41}$$

assuming Gaussian distributions and no correlation between A and τ. For CH_4, the relative uncertainty in τ is estimated to be 38 % (Prather et al., 2012, our conversion to 5–95 % confidence interval) and 20 % for A (Forster et al., 2007, our conversion to 5–95 % confidence interval). Using Eq. (41) with these uncertainties, the total uncertainty for $AGWP_{CH_4}$

is 31 % for a 20 yr time horizon (for 5–95 % confidence interval), 43 % for 100 yr, and 43 % for 500 yr, with twice as large contribution from the second term relative to the first term. The uncertainty in the $AGWP_{CO_2}$ can be obtained using the 20 % estimated uncertainty in RE (Forster et al., 2007, our conversion to 5–95 % confidence interval) and uncertainty in the integrated IRF_{CO_2} of 29, 49, and 56 % (for 5–95 % confidence interval) for a 20, 100, and 500 yr time horizon (Joos et al., 2013). The uncertainty for a product (i.e., $RE_{CO_2} \times \int IRF_{CO_2}$), in this case $AGWP_{CO_2}$, is given by

$$\frac{\Delta AGWP_{CO_2}}{AGWP_{CO_2}} = \sqrt{\left(\frac{\Delta RE_{CO_2}}{RE_{CO_2}}\right)^2 + \left(\frac{\Delta \int IRF_{CO_2}}{\int IRF_{CO_2}}\right)^2} \quad (42)$$

leading to an uncertainty of $AGWP_{CO_2}$ of 35, 53, and 59 % (for 5–95 % confidence interval), respectively, with the uncertainty dominated by the uncertainty in the integrated IRF_{CO_2}. Combining the relative uncertainty in the $AGWP_{CH_4}$ and $AGWP_{CO_2}$ (using the sum of the squares uncertainty propagation), the uncertainty in GWP_{CH_4} is 47, 68, and 73 % (for 5–95 % confidence interval) for a 20, 100, and 500 yr time horizon. The uncertainty is given by both, but with an overweight on $AGWP_{CO_2}$ for the longer time horizons. The uncertainties we find are similar to those reported in other studies (Reisinger et al., 2010; Boucher, 2012). The simple analysis described here gives a general idea of the uncertainty in GWP_{CH_4} and highlights which terms contribute most to the uncertainty.

Irrespective of the uncertainties, the effect of choice of metric and time horizon is generally larger than the uncertainties. For example, Reisinger et al. (2010) find that the GWP_{CH_4} is between 55–93 (90 % range) for a 20 yr time horizon, 17–35 for a 100 yr time horizon, and the GTP_{CH_4} is between 4–15 for 100 yr. In addition, the decision on which indirect effects to include can also change metric values, e.g., Shindell et al. (2009) find that the GWP_{CH_4} increases from 25 to 34 by including indirect effects of aerosols. Thus, while the scientific uncertainties are large and need to be reduced, larger variations are due to value judgments. This further emphasises the importance of a clear definition of each metric and ensuring that impact assessment studies are robust to the choice of metric by exploring results for a range of metrics.

5 Methods for sustained emissions and emission scenarios

Pulse emissions are used due to their simplicity and generality. The response of a pulse emission can be seen as the building block of the response for an emission scenario through the use of convolutions (Enting, 2007; Wigley, 1991). A particular type of scenario often used in emission metrics is a sustained emission which assumes emissions continue indefinitely at a pre-defined level. In this section, we discuss how emission metrics for pulse emissions can be applied in more general situations; first, for the specific case of sustained emissions, and second in the more general case.

5.1 Sustained emissions

A simple "emission scenario" is to have continuous (or sustained) emissions. The absolute metric of a sustained emission can be calculated as the integral of the absolute metric of a pulse emission. Sustained emissions are a specific type of scenario that neglects changes due to economic growth, technology improvements, mitigation policies, or the lifecycle of infrastructure. It is often assumed for simplicity that sustained emissions do not change the background concentrations (as for pulse emissions, they are marginal); hence, all factors influencing the metric calculations stay constant. From a policy perspective, sustained emission may seem more relevant, since in reality, emissions are unlikely to stop instantaneously as in a pulse emission. However, from a scientific perspective, processes easily observable in a pulse emission can be masked by a sustained emission. The choice between a pulse and sustained emission scenario for a mix of species is an important value judgment as they place very different weights on SLCFs and LLGHGs.

In the following, we show the equations for the different metrics with sustained emissions. The RF for species with a simple exponential decay and sustained emission is

$$RF_{x,s}(H) = A_x \tau \left(1 - \exp\left(-\frac{H}{\tau}\right)\right) \quad (43)$$

This equation is identical to the AGWP for a pulse emission. The AGWP for a sustained emission is

$$AGWP_{x,s}(H) = A_x \tau \left[H - \tau \left(1 - \exp\left(-\frac{H}{\tau}\right)\right)\right] \quad (44)$$

The AGTP for a sustained emission is

$$AGTP_{x,s}(H) = \sum_{j=1}^{J} A_x \tau \lambda \left(1 - \exp\left(-\frac{H}{d_j}\right)\right) + AGTP_x(H) \quad (45)$$

And finally, the iAGTP for a sustained emission is

$$iAGTP_{x,s}(H) = \sum_{j=1}^{J} A_x \tau \lambda \left(H - d_j \left(1 - \exp\left(-\frac{H}{d_j}\right)\right)\right) + iAGTP_x(H) \quad (46)$$

Similar equations can be derived for CO_2 and ozone precursors, but are not shown here in the interest of space.

There is a close connection between pulse and sustained emission metrics as eluded to earlier. A property of convolutions with a linear response and the Heaviside step function (equivalent to a sustained emission), can be used to show that the RF of a sustained emission (RF_s, left hand side) is equal to the integrated RF of a pulse emission (AGWP, right hand side),

$$RF_{x,s}(t) = \int_0^t H(s)\, R_x(t-s)\, ds = \int_0^t R_x(s)\, ds = \int_0^t RF_{x,p}(s)\, ds = AGWP_x(t) \quad (47)$$

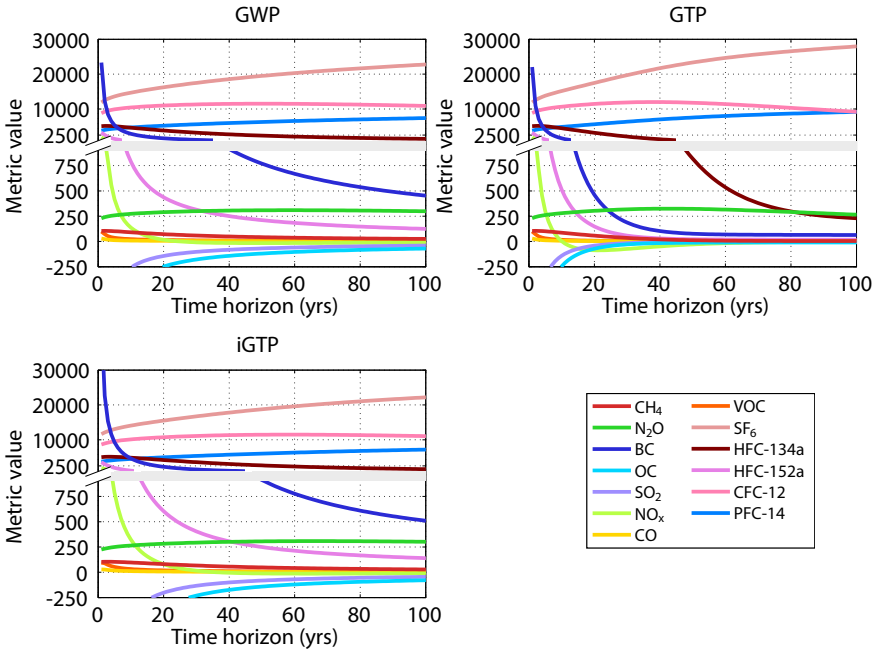

Fig. 8. GWP, GTP, and iGTP values for a range of pollutants and time horizons, the split in the vertical axis represents a change of scale at 900. The variable time horizon for these metrics GWP(H-t), GTP(H-t), and iGTP(H-t), are found by reversing the time horizon axis.

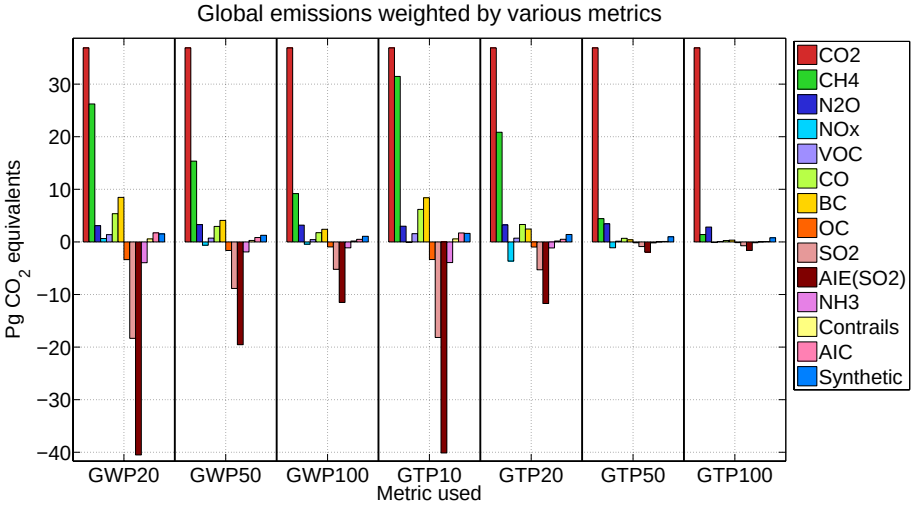

Fig. 9. The weighting of the different emissions from 2008, with BC and OC data from 2005, using various emission metrics.

Further, the same is true for a linear temperature response,

$$\Delta T_{x,\mathrm{s}}(t) = \int_0^t \mathrm{RF}_{x,\mathrm{s}}(s)\, R_T(t-s)\,\mathrm{d}s = \int_0^t \mathrm{AGWP}_x(s)\, R_T(t-s)\,\mathrm{d}s = \mathrm{iAGTP}_x(t) \quad (48)$$

so that the instantaneous temperature perturbation to a sustained emission is equal to the integrated temperature perturbation to a pulse emission. Thus, there is a close connection between pulse and sustained emission metrics; the instantaneous impact of a sustained emission is the same as the integrated impact of a pulse emission. In early work, Shine et al. (2005b) noted that the GWP was similar to the instantaneous temperature response to a sustained emission. This is equivalent to the integrated temperature response of a pulse emissions, and this has been shown to be similar to the GWP (Peters et al., 2011a; Azar and Johansson, 2012), thus, confirming the findings of Shine et al. (2005b).

Table 3. A list of all gases, particles, and indirect effects that are included in the sample applications presented. For each species, the literature that is used for input is given.

Species	Calculations based on
CO_2, CH_4, N_2O, HCFC-141b, HCF-142b, HFC-23, HFC-32, HFC-125, HFC-134a, HFC-143a, HFC-152a, HFC-227ea, HFC-236fa, HFC-245fa, HFC-365mfc, HFC-43-10mee, SF6, NF3, PFC-14, PFC-116, PFC-218, PFC-318, PFC-3-1-10, PFC-4-1-12, PFC-5-1-14, PFC-6-1-16	Forster et al. (2007)
BC, OC, SO_2, contrail, aircraft induced cirrus	Fuglestvedt et al. (2010)
Aircraft NO_x	Stevenson et al. (2004), as given by Fuglestvedt et al. (2010)
Surface NO_x	The global run in Wild et al. (2001), as given by Fuglestvedt et al. (2010)
Shipping NO_x	Fuglestvedt et al. (2008)
CO	Derwent et al. (2001), as given by Fuglestvedt et al. (2010)
VOC	Collins et al. (2002), as given by Fuglestvedt et al. (2010)
NH_3	Shindell et al. (2009)
AIE(SO_2)	1.75*SO_2, Forster et al. (2007)
Shipping AIE (SO_2)	8.3*SO_2. Average of Lauer et al. (2007), as given by Fuglestvedt et al. (2010)

5.2 General emission scenarios

For emission scenarios, the RF, AGWP, AGTP, and iAGTP values can be calculated with a convolution,

$$(f \times g)(t) = \int_{-\infty}^{\infty} f(s)\, g(t-s)\, \mathrm{d}s \tag{49}$$

where f and g are functions and g represents the emission metric for a pulse emission. For instance, the temperature response for a scenario is the convolution of the emission scenario and AGTP for a pulse emission:

$$\Delta T_i(t) = \int_0^t E_i(\tau)\, \mathrm{AGTP}_i(t-\tau)\, \mathrm{d}\tau \tag{50}$$

In this case, the AGTP is an IRF representing the link from emissions to temperature (IRF_T is the link from forcing to temperature). The convolution can be estimated by numerical integration, though, most numerical integrations have problems with species with a short lifetime (e.g., BC), typically when the time step is larger than the residence time ($\Delta t > \tau$). This problem can be solved by reducing the time step.

If the IRF is based on a sum of exponentials, then the convolution can be written as an equivalent ordinary differential equation (ODE) (Wigley, 1991).

$$\frac{\mathrm{d}F(H)}{\mathrm{d}t} = \sum_{k=1}^{K} \frac{\mathrm{d}F_k(H)}{\mathrm{d}t} = E(H) \sum_{k=1}^{K} \alpha_k - \sum_{k=1}^{K} \frac{F_k}{\tau_k} \tag{51}$$

The ODE can be solved numerically and we find this to be a more robust and efficient method than the direct estimation of the convolution numerically. This method requires a response based on exponential functions and, thus, cannot be applied directly to emission metrics as in Eq. (50). However, a step-wise series of convolutions and integrations can perform the necessary calculations; for example, the RF can be determined using this method with integration leading to the integrated RF.

6 Sample applications

In this section, we present some specific and policy relevant applications using the emission metrics described above. The emission metrics presented in this article are based on simple parameterisations of more complex models (e.g., the global mean temperature response from Hadley CM3 is reduced to four parameters) and so the metric values only approximate the actual responses.

6.1 Data and assumptions

As input data, we use the 2008 emissions from the Emissions Database for Global Atmospheric Research (EDGAR) (EC, 2011), with the exception of BC and OC from 2005 (Shindell et al., 2012). BC and OC emissions from biomass burning are not included, in contrast to e.g. Lamarque et al. (2010). Although new input exists for some species, we prefer to use values that are consistent with those given by IPCC (2007)

Table 4. The top ten emitting countries according to different emission metrics. The percentage given is the share of the global sum.

Ranking of emitters by metrics	GWP20	GWP100	GTP20	GTP50	GTP100
1	US 30.1 %	China 17.1 %	China 17.5 %	China 20.3 %	China 20.6 %
2	Brazil 10.1 %	US 16.7 %	US 14.8 %	US 14.5 %	US 14.9 %
3	Russia 9.7 %	Russia 5.9 %	Russia 6.1 %	Russia 5.3 %	Russia 5.3 %
4	Indonesia 9.5 %	Indonesia 5.1 %	India 5.6 %	India 4.8 %	India 4.5 %
5	India 5.8 %	India 4.9 %	Indonesia 4.7 %	Indonesia 4.4 %	Indonesia 4.5 %
6	Germany 4.5 %	Brazil 3.9 %	Brazil 4.4 %	Japan 3.1 %	Japan 3.3 %
7	Japan 4.5 %	Japan 3.3 %	Japan 2.7 %	Brazil 3.0 %	Brazil 2.7 %
8	France 3.1 %	Germany 2.6 %	Germany 2.2 %	Germany 2.3 %	Germany 2.4 %
9	UK 3.0 %	UK 1.6 %	Canada 1.5 %	Canada 1.5 %	Canada 1.5 %
10	Nigeria 2.8 %	Canada 1.6 %	Mexico 1.4 %	UK 1.4 %	UK 1.4 %

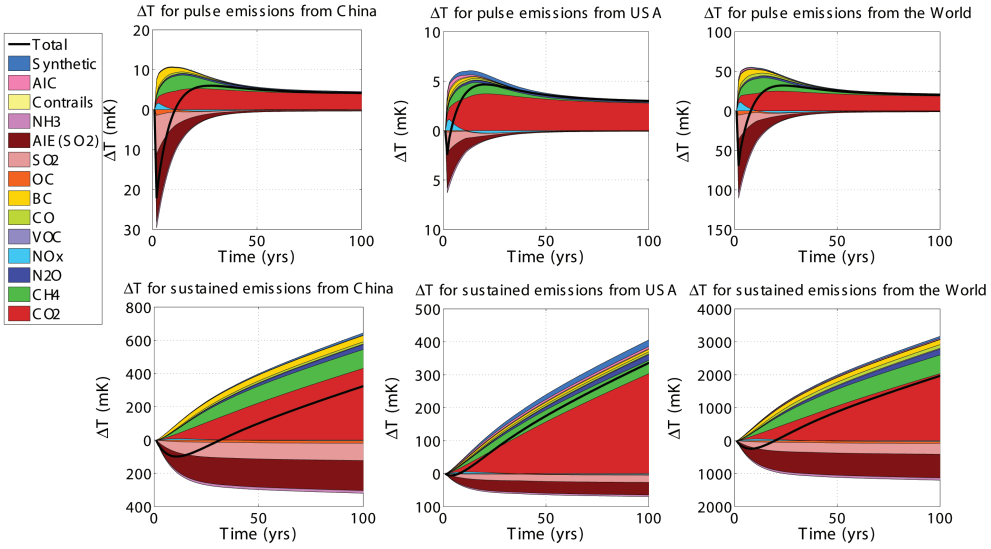

Fig. 10. The estimated temperature perturbation based on AGTP by different species due to EDGAR 2008 emissions. "Synthetic" represents the mainly halogenated hydrocarbons in the Kyoto and Montreal Protocols.

and the ATTICA assessment (Fuglestvedt et al., 2010). The parameters used in the metrics presented here can be found in Forster et al. (2007); Fuglestvedt et al. (2010).

The IRF for CO_2 is based on the Bern Carbon Cycle Model (Joos et al., 2001) as reported in Forster et al. (2007), and a recent model intercomparison shows that the Bern model is likely to be close to the model mean (Joos et al., 2013, Fig. 1). The IRF for temperature is based on the Hadley CM3 climate model (Boucher and Reddy, 2008), and a recent model comparison shows that the Hadley IRF lies within the 5–95 % range in a model intercomparison (Olivié and Peters, 2012). The remaining RE and lifetimes for the long-lived greenhouse gases are from Forster et al. (2007), for BC, OC, direct SO_2, contrail, and aircraft induced cirrus from Fuglestvedt et al. (2010). The parameters for aircraft NO_x are from Stevenson et al. (2004), for surface NO_x the global run from Wild et al. (2001), for shipping NO_x from Fuglestvedt et al. (2008), for CO from Derwent et al. (2001), and for VOC from Collins et al. (2002), as given by Fuglestvedt et al. (2010). Since Collins et al. (2002) give the metric parameterizations for VOC per unit C and not VOC, the emissions from EDGAR have been multiplied with a factor of 0.6 (IPCC, 2006). The metric values for NH_3 are based on Shindell et al. (2009). The BC parameterisation here does not consider the impact of BC in snow (see Sect. 2.3.3). An overview of species included and references used is given in Table 3.

The aerosol indirect effect (AIE) is normally applied in the metrics by scaling it relative to the direct (sulfate) aerosol effect. The scaling is obtained using globally averaged central estimate values and is crudely set to 1.5–2, as the AIE is larger than the direct aerosol effect. The direct aerosol effect and indirect aerosol effect have radiative forcings of about -0.5 and $-0.7\,\mathrm{W\,m^{-2}}$, respectively (Forster et al., 2007). However, many different aerosols can lead to the AIE, and

it is currently not possible to attribute the total AIE to the various types of aerosols. Our default case is to assume the AIE is entirely due to SO_2. We have scaled AIE in shipping as the indirect effect of SO_2 given by the average of Lauer et al. (2007), which scales AIE to be 830 % of the direct effect. For all other sectors, the AIE can be estimated to be about 175 % of the direct effect of SO_2 (Forster et al., 2007). We have also tested a variety of other cases to see how the AIE may vary if it is due to a mix of aerosols. In one case, we based the AIE on a mix of BC (10 %), OC (30 %) and SO_2 (60 %) to test the robustness of the ranking given the ranges for AIE. The ranking of sectors for global emissions differs little between the parameterisations, and these variations are only observed for the shortest time horizons.

6.2 Metric values as a function of time horizon

The GWP, GTP and iGTP values for a range of pollutants are shown in Fig. 8 based on equations in Sects. 3.1.2, 3.1.3 and 3.1.4. The metric values for a few selected time horizons are available in Forster et al. (2007) and Fuglestvedt et al. (2010). Since both GWP and iGTP integrate the effects over time, both these metrics integrate all of the climate effects that occurred at previous times, while the GTP puts less weight on the RF at earlier times as the ocean modulates the transport of energy radiated back to space. GTP is an end-point metric that only looks at the climate system at a specific time. As shown in earlier work, there is a similarity between the GWP and iGTP, but neither is similar to the GTP (Peters et al., 2011a). The GTP values are generally lower for the same time horizon. Organic carbon (OC) and SO_2 have negative RF and, hence, negative metric values for all times. NO_x has a net value that is initially positive and, then, change sign as different responses take effect. Almost all species become less important with time relative to CO_2, with the exception of N_2O and other LLGHGs with similar or longer lifetimes. For N_2O, it takes about 50 yr before its GTP value begins to decrease.

It is also possible to have metrics with a variable time horizon, where the evaluation year (TE) is fixed and the time horizon is reduced as the evaluation year is approaching, $\mathrm{TH}(t) = \mathrm{TE}\text{-}t$ (Shine et al., 2007). Metrics with such a variable time horizon can be visualised as the mirror image of Fig. 8 (along the time horizon axis), also see Fig. 1 in Shine et al. (2007). As the evaluation year is approached, the metric values of species with lifetimes similar to CH_4 and shorter increase. For the other LLGHGs, the metric values are rather constant throughout the period.

6.3 Ranking of countries by total emissions using different metrics

Figure 9 shows the CO_2-equivalent emissions for global emissions in 2008, including both SLCFs and LLGHGs, and using different emission metrics. The importance of the SLCFs decreases with increasing time horizon and their relative contributions are small when using a GTP with a 100 yr time horizon. CO_2 dominates the metric weighted emissions in all cases, even when GTP20 is used. For the shortest time horizons, the effect of the sum of SO_2 and AIE can be larger than the effect of CO_2.

In Table 4, we rank countries according to climate impact by using different emission metrics. There are few changes in ranking with the use of different emission metrics since CO_2 emissions dominate the total climate response, with the exception of GWP20. The relative share of global emissions attributed to individual countries can differ; China's share of global emissions varies between 17 and 21 % using the GWP100 and GTP100, while China's share is negligible for GWP20. A key reason for the differences using a GWP20 is that the metric values of SLCFs change rapidly for small times; for instance, the cooling from SO_2 and AIE is significant with GWP20 and SO_2 emissions vary significantly between countries. The top ten emitters are almost independent of the metric, with the exception of GWP20.

Within each country, the relative weights of SLCFs and LLGHGs can change significantly with different metrics. Table 5 shows the relative share of CH_4 in the total emissions using different emission metrics for the top ten emitters (as for GWP100). The share attributed to methane decreases with time horizon, as CH_4 has a much shorter response time than CO_2. Many developing countries have relative large CH_4 emissions and are particularly affected by changing metrics. Using a GWP100, CH_4 represents about 36 and 41 % of the total emissions in Brazil and India, respectively, but this increases to about 56 and 63 % with GTP20. China and the Russian Federation have 30 and 29 % allocated to CH_4 for a GWP100, but increasing to 51 and 49 % with

Table 5. The share of methane relative to the total emissions for top ten emitters when using different emission metrics. Due to the strong negative climate response (cooling) of SLCFs in some countries, the shares of CH_4 can be greater than 100 % for some metrics with short time horizons. This is not due to CH_4 dominating the total climate impact, but due to cancelation effects between warming and cooling effects (see Fig. 10). For China, there is a net cooling for GWP20; thus, a methane share is not available.

Share of methane for countries	GWP20	GWP100	GTP20	GTP50	GTP100
China	N/A	29.7 %	51.2 %	10.2 %	3.4 %
US	31.7 %	10.8 %	21.7 %	5.1 %	1.7 %
Russia	91.6 %	28.5 %	48.8 %	12.9 %	4.4 %
India	182.2 %	41.2 %	62.8 %	17.2 %	6.1 %
Indonesia	39.7 %	13.9 %	26.7 %	6.6 %	2.2 %
Japan	16.3 %	4.1 %	8.7 %	1.8 %	0.6 %
Brazil	72.7 %	35.9 %	56.2 %	19.1 %	7.1 %
Germany	22.5 %	7.3 %	15.4 %	3.4 %	1.1 %
Canada	111.5 %	22.9 %	41.1 %	9.5 %	3.2 %
UK	35.0 %	12.4 %	25.1 %	5.9 %	1.9 %

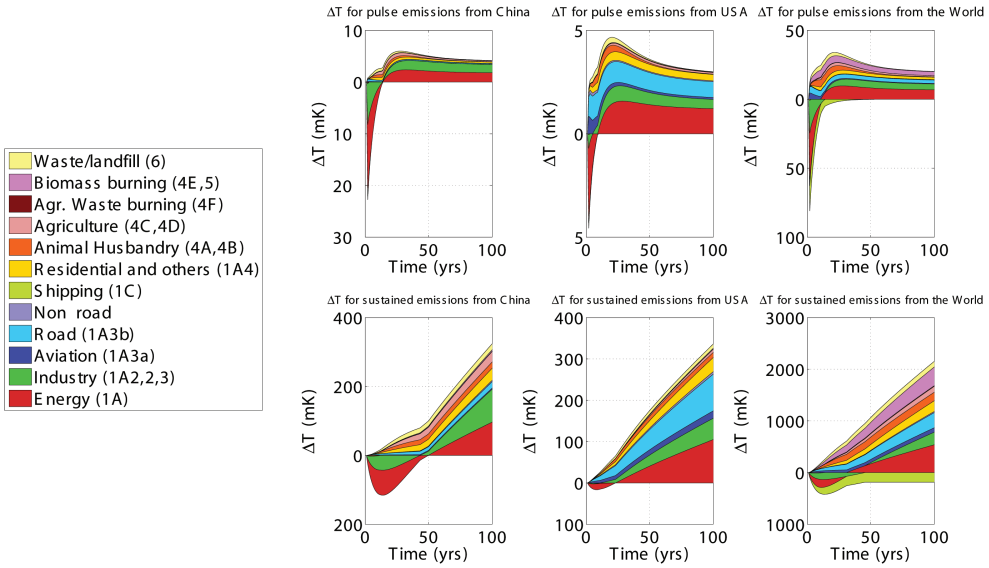

Fig. 11. The estimated temperature perturbation based on AGTP for different sectors due to EDGAR 2008 emissions. The net result (sum of all sectors) is found Fig. 10.

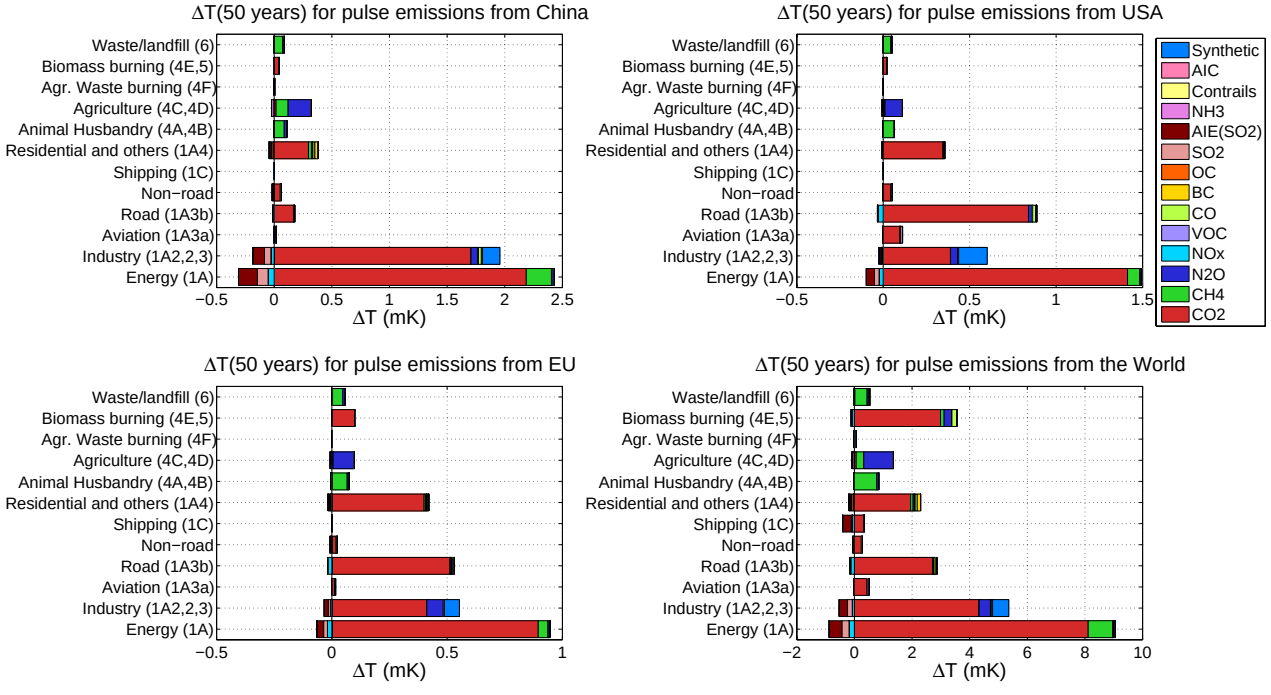

Fig. 12. The estimated temperature perturbation based on AGTP 50 yr after EDGAR 2008 emission for different sectors. For a shorter time horizon, the non-CO_2 effects will be relative larger compared to CO_2. "Synthetic" represents the mainly halogenated hydrocarbons in the Kyoto and Montreal Protocols. BC and OC emissions from biomass burning are not included.

GTP20. The contribution of CH_4 is largest for GWP20 due to the shorter perturbation lifetime of CH_4, and for GWP20 the contribution of CH_4 can be greater than 100 % due to the presence of SLCFs with cooling effects. Thus, changing emission metric may have a significant impact on the distribution of emissions allocated to each country, and consequently, this may have significant effects on calculated mitigation costs and ranking of measures.

6.4 Application of metrics to sectorial and regional emissions

Figure 10 shows the estimated temperature perturbation based on time dependent AGTP as calculated by Eq. (49) for pulse and sustained emissions of EDGAR year 2008 according to species for China, the USA and globally. The sustained emission scenario assumes constant 2008 emissions into the future, and we further assume – consistent with the application of metrics (to compare GHGs) – that this does not affect the background concentration. While the SLCFs are important for the temperature perturbation in the first years after a pulse emission, CO_2 dominates in the long run, which is due to long response time for CO_2. In general, the climate impact is governed by species with strong, but short-lived impact and weak, but long-lived impacts. In the sustained emission case, the emissions continue into the atmosphere indefinitely; hence, the temperature perturbation from SLCFs is not reduced as time increases, but instead reaches approximately a steady-state. However, the concentration of CO_2 increases with time as it does not decay to zero and, thus, accumulates in the atmosphere, leading to a near linear increase in the temperature perturbation from CO_2 emissions. The differences between countries are rather small.

The same estimated temperature perturbation is divided according to sectors in Fig. 11. Instantaneous pulse emissions for 2008 emissions from all sectors give rise to warming, with the exception of cooling from the energy and industry sectors in the first 5–20 yr and a small cooling from shipping in the first 40 yr. The cooling is due to emissions of SO_2 and is more persistent in China due to the higher emissions of SO_2 relative to CO_2. If we exclude the AIE, the cooling occurs only in the first 5 yr for the energy and industry sectors and between year 10 and 30 for shipping. In the long run, the energy and industry sectors have the largest perturbation for both pulse and sustained emissions, as CO_2 dominates over the cooling components. Only the shipping sector has a continuous negative contribution in the sustained case; however, note that this assumes no changes in emissions or technology into the future.

While Figs. 10 and 11 consider emissions by species and sector separately as a function of time; Fig. 12 shows the contribution of the different sectors by species after 50 yr for China, USA, EU and the World. Globally, the largest sectors according to AGTP50 are energy , industry, biomass burning and road transportation. CO_2 has overall the largest impact, while CH_4 dominates the sectors animal husbandry and waste and N_2O dominates agriculture. Emissions of synthetic gases come mainly from the industry sector.

7 Conclusions

We have presented the parameterisations and analytical expressions of radiative forcing, integrated radiative forcing, temperature and integrated temperature change in both absolute and normalised forms for three types of species: (1) species with a simple exponential decay (e.g., CH_4), (2) CO_2 which has a complex decay over time, and 3) ozone precursors (e.g., NO_x, CO, VOC). Since the purpose of using metrics differs depending on context and the questions being addressed, different metrics and time horizons may be preferable for different applications. We have discussed key issues and assumptions in the various parameterisations, particularly in relation to deriving Impulse Response Functions, radiative efficiencies, lifetimes, and a range of indirect effects. Finally, we applied the metrics in a variety of different applications to show the importance of metrics and the related choices in policy-relevant applications, such as ranking of emissions from countries, sectors and different species. We have focused on simple reduced form emission metrics based on simple analytical expressions with parameters derived from more complex models. There are a range of alternative approaches to develop emission metrics that include more detailed representations of the climate or economic system. The sample applications show that CO_2 is important regardless of what metric and time horizon is used, but that the importance of SLCFs varies greatly depending on the metric used. The ranking of the top ten countries by emissions varies little with different metrics (except for GWP20). We hope that this document acts as a valuable documentation for future metrics calculations, comparisons, further development and will be useful for various applications.

Acknowledgements. The authors would like to acknowledge the support from the Norwegian Research Council projects: Transport and Environment – Measures and POlicies (TEMPO) and Climate and health impacts of Short Lived Atmospheric Components (SLAC). In addition, the research leading to these results has received funding from the European Union Seventh Framework Programme (FP7/2007-2013) under grant agreement no 282688 – ECLIPSE. We thank Gunnar Myhre, Terje Berntsen, Marianne T. Lund, and Bjørn Samset for comments and Zbigniew Klimont for providing BC and OC emission datasets. Further, we thank Robbie Andrew for help with some of the figures. We thank François-Marie Bréon for identifying an error in an early version of the paper. We also appreciate the valuable comments given by Daniel Johansson, an anonymous referee, and the editor.

Edited by: S. Smith

References

Archer, D. and Brovkin, V.: The millennial atmospheric lifetime of anthropogenic CO_2, Climatic Change, 90, 283–297, doi:10.1007/s10584-008-9413-1, 2008.

Archer, D., Eby, M., Brovkin, V., Ridgwell, A., Cao, L., Mikolajewicz, U., Caldeira, K., Matsumoto, K., Munhoven, G., Montenegro, A., and Tokos, K.: Atmospheric lifetime of fossil fuel carbon dioxide, in: Annual review of earth and planetary sciences, Annual review of earth and planetary sciences, Ann. Rev., Palo Alto, 117–134, 2009.

Azar, C. and Johansson, D. J. A.: On the relationship between metrics to compare greenhouse gases –the case of IGTP, GWP and SGTP, Earth Syst. Dynam., 3, 139–147, doi:10.5194/esd-3-139-2012, 2012.

Berntsen, T. and Fuglestvedt, J. S.: Global temperature responses to current emissions from the transport sectors, Proc. Natl. Acad. Sci., 105, 19154–19159, doi:10.1073/pnas.0804844105, 2008.

Berntsen, T., Fuglestvedt, J. S., Joshi, M., Shine, K., Stuber, N., Li, L., Hauglustaine, D., and Ponater, M.: Climate response to regional emissions of ozone precursers: Sensitivities and warming potentials, Tellus B, 57, 283–304, 2005.

Berntsen, T., Fuglestvedt, J. S., Myhre, G., Stordal, F., and Berglen, T. F.: Abatement of greenhouse gases: Does location matter?, Climatic Change, 74, 377–411, 2006.

Boer, G. B. and Yu, B. Y.: Climate sensitivity and response, Clim. Dynam., 20, 415–429, doi:10.1007/s00382-002-0283-3, 2003.

Bond, T. C., Zarzycki, C., Flanner, M. G., and Koch, D. M.: Quantifying immediate radiative forcing by black carbon and organic matter with the Specific Forcing Pulse, Atmos. Chem. Phys., 11, 1505–1525, doi:10.5194/acp-11-1505-2011, 2011.

Boucher, O.: Comparison of physically- and economically-based CO_2-equivalences for methane, Earth Syst. Dynam., 3, 49–61, doi:10.5194/esd-3-49-2012, 2012.

Boucher, O. and Reddy, M. S.: Climate trade-off between black carbon and carbon dioxide emissions, Energ. Pol., 36, 193–200, 2008.

Boucher, O., Friedlingstein, P., Collins, B., and Shine, K. P.: The indirect global warming potential and global temperature change potential due to methane oxidation, Environ. Res. Lett., 4, 044007, doi:10.1088/1748-9326/4/4/044007, 2009.

Caldeira, K. and Kasting, J. F.: Insensitivity of global warming potentials to carbon dioxide emission scenarios, Nature, 366, 251–253, 1993.

Collins, W. J., Derwent, R. G., Johnson, C. E., and Stevenson, D. S.: The oxidation of organic compounds in the troposphere and their global warming potentials, Climatic Change, 52, 453–479, doi:10.1023/a:1014221225434, 2002.

Collins, W. J., Sitch, S., and Boucher, O.: How vegetation impacts affect climate metrics for ozone precursors, J. Geophys. Res., 115, D23308, doi:10.1029/2010jd014187, 2010.

Collins, W. J., Fry, M. M., Yu, H., Fuglestvedt, J. S., Shindell, D. T., and West, J. J.: Global and regional temperature-change potentials for near-term climate forcers, Atmos. Chem. Phys., 13, 2471–2485, doi:10.5194/acp-13-2471-2013, 2013.

Cox, R. A. and Wuebbles, D.: Scientific assessment of stratospheric ozone: 1989. Volume 1, Chapter 4. Halocarbon ozone depletion and global warming potentials, World Meteorological Organization, Geneva, Switzerland, 1989.

Daniel, J. S., Solomon, S., and Albritton, D. L.: On the evaluation of halocarbon radiative forcing and global warming potentials, J. Geophys. Res., 100, 1271–1285, doi:10.1029/94jd02516, 1995.

Daniel, J., Solomon, S., Sanford, T., McFarland, M., Fuglestvedt, J., and Friedlingstein, P.: Limitations of single-basket trading: Lessons from the montreal protocol for climate policy, Climatic Change, 111, 241–248, doi:10.1007/s10584-011-0136-3, 2012.

Denman, K. L., Brasseur, G., Chidthaisong, A., Ciais, P., Cox, P. M., Dickinson, R. E., Hauglustaine, D., Heinze, C., Holland, E., Jacob, D., Lohmann, U., Ramachandran, S., Dias, P. L. D. S., Wofsy, S. C., and Zhang, X.: Couplings between changes in the climate system and biogeochemistry, in: Climate change 2007: The physical science basis. Contribution of working group i to the fourth assessment report of the intergovernmental panel on climate change, edited by: Solomon, S. D., Qin, D., Manning, M., Chen, Z., Marquis, M., Averyt, K. B., Tignor, M., and Miller, H. L., Cambridge University Press, Cambridge, United Kingdom and New York, NY, USA, 2007.

Derwent, R. G., Environmental, U. K. A. E. A., and Division, M. S.: Trace gases and their relative contribution to the greenhouse effect, AEA Technology, Atomic Energy Research Establishment, 1990.

Derwent, R. G., Collins, W. J., Johnson, C. E., and Stevenson, D. S.: Transient behaviour of tropospheric ozone precursors in a global 3-D CTM and their indirect greenhouse effects, Climatic Change, 49, 463–487, doi:10.1023/a:1010648913655, 2001.

Doherty, S. J., Warren, S. G., Grenfell, T. C., Clarke, A. D., and Brandt, R. E.: Light-absorbing impurities in Arctic snow, Atmos. Chem. Phys., 10, 11647–11680, doi:10.5194/acp-10-11647-2010, 2010.

Eby, M., Zickfeld, K., Montenegro, A., Archer, D., Meissner, K. J., and Weaver, A. J.: Lifetime of anthropogenic climate change: Millennial time scales of potential CO_2 and surface temperature perturbations, J. Climate, 22, 2501–2511, doi:10.1175/2008jcli2554.1, 2009.

EC: Emission database for global atmospheric research (EDGAR), release version 4.2., edited by: European Commission, J. R. C. J. N. E. A. A. P., available at: http://edgar.jrc.ec.europa.eu/ (last access: 26 April 2013), 2011.

Enting, I. G.: Laplace transform analysis of the carbon cycle, Environ. Modell. Softw., 22, 1488–1497, doi:10.1016/j.envsoft.2006.06.018, 2007.

Enting, I. G., Wigley, T. M. L., and Heimann, M.: Future emissions and concentrations of carbon dioxide: Key ocean/atmosphere/land analyses, CSIRO Division of Atmospheric Research Technical Paper no. 31, 1994.

Forster, P., Ramaswamy, V., Artaxo, P., Berntsen, T., Betts, R., Fahey, D. W., Haywood, J., Lean, J., Lowe, D. C., Myhre, G., Nganga, J., Prinn, R., Raga, G., Schulz, M., and Dorland, R. V.: Changes in atmospheric constituents and in radiative forcing, in: Climate change 2007: The physical science basis. Contribution of working group i to the fourth assessment report of the intergovernmental panel on climate change, edited by: Solomon, S., Qin, D., Manning, M., Chen, Z., Marquis, M., Averyt, K. B., Tignor, M., and Miller, H. L., Cambridge University Press, Cambridge, United Kingdom and New York, NY, USA, 2007.

Friedlingstein, P., Cox, P., Betts, R., Bopp, L., von Bloh, W., Brovkin, V., Cadule, P., Doney, S., Eby, M., Fung, I., Bala, G., John, J., Jones, C., Joos, F., Kato, T., Kawamiya, M., Knorr,

W., Lindsay, K., Matthews, H. D., Raddatz, T., Rayner, P., Reick, C., Roeckner, E., Schnitzler, K. G., Schnur, R., Strassmann, K., Weaver, A. J., Yoshikawa, C., and Zeng, N.: Climate–carbon cycle feedback analysis: Results from the C4MIP model intercomparison, J. Climate, 19, 3337–3353, doi:10.1175/jcli3800.1, 2006.

Fry, M. M., Naik, V., West, J. J., Schwarzkopf, D., Fiore, A., Collins, W. J., Dentener, F., Shindell, D. T., Atherton, C. S., Bergmann, D. J., Duncan, B. N., Hess, P. G., MacKenzie, I. A., Marmer, E., Schultz, M. G., Szopa, S., Wild, O., and Zeng, G.: The influence of ozone precursor emissions from four world regions on tropospheric composition and radiative climate forcing, J. Geophys. Res., 117, D07306, doi:10.1029/2011JD017134, 2012.

Fuglestvedt, J. S., Isaksen, I. S. A., and Wang, W. C.: Estimates of indirect global warming potentials for CH_4, CO and NO_x, Climatic Change, 34, 405–437, 1996.

Fuglestvedt, J. S., Berntsen, T. K., Isaksen, I. S. A., Mao, H., Liang, X.-Z., and Wang, W.-C.: Climatic forcing of nitrogen oxides through changes in tropospheric ozone and methane; global 3D model studies, Atmos. Environ., 33, 961–977, doi:10.1016/s1352-2310(98)00217-9, 1999.

Fuglestvedt, J. S., Berntsen, T., Godal, O., and Skovdin, T.: Climate implications of GWP-based reductions in greenhouse gas emissions, Geophys. Res. Lett., 27, 409–412, 2000.

Fuglestvedt, J. S., Berntsen, T. K., Godal, O., Sausen, R., Shine, K. P., and Skodvin, T.: Metrics of climate change: Assessing radiative forcing and emission indices, Climatic Change, 58, 267–331, 2003.

Fuglestvedt, J., Berntsen, T., Myhre, G., Rypdal, K., and Skeie, R. B.: Climate forcing from the transport sectors, Proc. Natl. Acad. Sci., 105, 454–458, doi:10.1073/pnas.0702958104, 2008.

Fuglestvedt, J. S., Shine, K. P., Berntsen, T., Cook, J., Lee, D. S., Stenke, A., Skeie, R. B., Velders, G. J. M., and Waitz, I. A.: Transport impacts on atmosphere and climate: Metrics, Atmos. Environ., 44, 4648–4677, 2010.

Gillett, N. P. and Matthews, H. D.: Accounting for carbon cycle feedbacks in a comparison of the global warming effects of greenhouse gases, Environ. Res. Lett., 5, 034011, doi:10.1088/1748-9326/5/3/034011, 2010.

Hansen, J. and Nazarenko, L.: Soot climate forcing via snow and ice albedos, Proc. Natl. Acad. Sci. USA, 101, 423–428, doi:10.1073/pnas.2237157100, 2004.

Hansen, J., Sato, M., Ruedy, R., Nazarenko, L., Lacis, A., Schmidt, G. A., Russell, G., Aleinov, I., Bauer, M., Bauer, S., Bell, N., Cairns, B., Canuto, V., Chandler, M., Cheng, Y., Del Genio, A., Faluvegi, G., Fleming, E., Friend, A., Hall, T., Jackman, C., Kelley, M., Kiang, N., Koch, D., Lean, J., Lerner, J., Lo, K., Menon, S., Miller, R., Minnis, P., Novakov, T., Oinas, V., Perlwitz, J., Perlwitz, J., Rind, D., Romanou, A., Shindell, D., Stone, P., Sun, S., Tausnev, N., Thresher, D., Wielicki, B., Wong, T., Yao, M., and Zhang, S.: Efficacy of climate forcings, J. Geophys. Res., 110, D18104, doi:10.1029/2005jd005776, 2005.

Held, I. M.: The gap between simulation and understanding in climate modelling, B. Am. Meteorol. Soc., 86, 1609–1614, doi:10.1175/BAMS-86-11-1609, 2005.

Hendricks, J., Kärcher, B., and Lohmann, U.: Effects of ice nuclei on cirrus clouds in a global climate model, J. Geophys. Res., 116, D18206, doi:10.1029/2010JD015302, 2011.

Henze, D. K., Shindell, D. T., Akhtar, F., Spurr, R. J. D., Pinder, R. W., Loughlin, D., Kopacz, M., Singh, K., and Shim, C.: Spatially refined aerosol direct radiative forcing efficiencies, Environ. Sci. Technol., 46, 9511–9518, doi:10.1021/es301993s, 2012.

Hodnebrog, Ø., Etminan, M., Fuglestvedt, J. S., Marston, G., Myhre, G., Nielsen, C. J., Shine, K. P., and Wallington, T. J.: Global warming potentials and radiative efficiencies of halocarbons and related compounds: A comprehensive review, Rev. Geophys., doi:10.1002/rog.20013, accepted, 2013.

Huijbregts, M. A. J., Hellweg, S., and Hertwich, E.: Do we need a paradigm shift in life cycle impact assessment?, Environ. Sci. Technol., 45, 3833–3834, doi:10.1021/es200918b, 2011.

IPCC: Climate change: The IPCC scientific assessment, edited by: Houghton, J. T., Jenkins, G. J., and Ephraums, J. J., Cambridge University Press, Cambridge, UK, 1990.

IPCC: Radiative forcing of climate change and an evaluation of the IPCC IS92 emission scenarios, edited by: Houghton, J. T., Filho, L. G. M., Bruce, J., Lee, H., Callander, B. A., Haites, E., Harris, N., and Maskell, K., Cambridge University Press, UK, 1994.

IPCC: The science of climate change, edited by: Houghton, J. T., Meira Filho, L. G., Callender, B. A., Harris, N., Kattenberg, A., and Maskell , K., Cambridge University Press, Cambridge, UK, 1995.

IPCC: Climate Change 2001 – the scientific basis, Cambridge University Press, Cambridge, UK, 2001.

IPCC: IPCC guidelines for national greenhouse gas inventories, prepared by the national greenhouse gas inventories programme, edited by: Eggleston, H. S., Buendia, L., Miwa, K., Ngara, T., and Tanabe, K., IGES, Japan, 2006.

IPCC: Climate change 2007: The physical science basis. Contribution of working group i to the fourth assessment report of the intergovernmental panel on climate change, edited by: Solomon, S., D. Q., Manning, M., Chen, Z., Marquis, M., Averyt, K. B., Tignor, M., and Miller, H. L., Cambridge University Press, Cambridge, United Kingdom and New York, NY, USA, 2007.

IPCC: IPCC expert meeting on the science of alternative metrics, edited by: Plattner, G.-K., Stocker, T. F., Midgley, P., and Tignor, M., IPCC Working Group I Technical Support Unit, Bern, Switzerland, 2009.

Isaksen, I. S. A., Ramaswamy, V., Rodhe, H., and Wigley, T. M. L.: Radiative forcing of climate change, in: Climate change 1992: The supplementary report to the IPCC scientific assessment, Cambridge University Press, Cambridge, 47–68, 1992.

Jacobson, M. Z.: Strong radiative heating due to the mixing state of black carbon in atmospheric aerosols, Nature, 409, 695–697, doi:10.1038/35055518, 2001.

Jacobson, M. Z.: Short-term effects of controlling fossil-fuel soot, biofuel soot and gases, and methane on climate, arctic ice, and air pollution health, J. Geophys. Res., 115, D14209, doi:10.1029/2009jd013795, 2010.

Johansson, D.: Economics- and physical-based metrics for comparing greenhouse gases, Climatic Change, 110, 123–141, doi:10.1007/s10584-011-0072-2, 2012.

Joos, F., Bruno, M., Fink, R., Siegenthaler, U., Stocker, T. F., Le Quéré, C., and Sarmiento, J. L.: An efficient and accurate representation of complex oceanic and biospheric models of anthropogenic carbon uptake, Tellus B, 48, 397–417, doi:10.1034/j.1600-0889.1996.t01-2-00006.x, 1996.

Joos, F., Prentice, I. C., Sitch, S., Meyer, R., Hooss, G., Plattner, G.-K., Gerber, S., and Hasselmann, K.: Global warming feedbacks on terrestrial carbon uptake under the intergovernmental panel on climate change (IPCC) emission scenarios, Global Biogeochem. Cy., 15, 891–907, doi:10.1029/2000gb001375, 2001.

Joos, F., Roth, R., Fuglestvedt, J. S., Peters, G. P., Enting, I. G., von Bloh, W., Brovkin, V., Burke, E. J., Eby, M., Edwards, N. R., Friedrich, T., Frölicher, T. L., Halloran, P. R., Holden, P. B., Jones, C., Kleinen, T., Mackenzie, F. T., Matsumoto, K., Meinshausen, M., Plattner, G.-K., Reisinger, A., Segschneider, J., Shaffer, G., Steinacher, M., Strassmann, K., Tanaka, K., Timmermann, A., and Weaver, A. J.: Carbon dioxide and climate impulse response functions for the computation of greenhouse gas metrics: a multi-model analysis, Atmos. Chem. Phys., 13, 2793–2825, doi:10.5194/acp-13-2793-2013, 2013.

Kandlikar, M.: The relative role of trace gas emissions in greenhouse abatement policies, Energ. Pol., 23, 879–883, doi:10.1016/0301-4215(95)00108-u, 1995.

Kandlikar, M.: Indices for comparing greenhouse gas emissions: Integrating science and economics, Energ. Econom., 18, 265–281, 1996.

Lamarque, J.-F., Bond, T. C., Eyring, V., Granier, C., Heil, A., Klimont, Z., Lee, D., Liousse, C., Mieville, A., Owen, B., Schultz, M. G., Shindell, D., Smith, S. J., Stehfest, E., Van Aardenne, J., Cooper, O. R., Kainuma, M., Mahowald, N., McConnell, J. R., Naik, V., Riahi, K., and van Vuuren, D. P.: Historical (1850–2000) gridded anthropogenic and biomass burning emissions of reactive gases and aerosols: methodology and application, Atmos. Chem. Phys., 10, 7017–7039, doi:10.5194/acp-10-7017-2010, 2010.

Lashof, D. A. and Ahuja, D. R.: Relative contributions of greenhouse gas emissions to global warming, Nature, 344, 529–531, 1990.

Lauer, A., Eyring, V., Hendricks, J., Jöckel, P., and Lohmann, U.: Global model simulations of the impact of ocean-going ships on aerosols, clouds, and the radiation budget, Atmos. Chem. Phys., 7, 5061–5079, doi:10.5194/acp-7-5061-2007, 2007.

Lelieveld, J. and Crutzen, P. J.: Indirect chemical effects of methane on climate warming, Nature, 355, 339–342, 1992.

Li, S. and Jarvis, A.: Long run surface temperature dynamics of an A-OGCM: The HadCM3 4×CO_2 forcing experiment revisited, Clim. Dynam., 33, 817–825, doi:10.1007/s00382-009-0581-0, 2009.

Li, S., Jarvis, A. J., and Leedal, D. T.: Are response function representations of the global carbon cycle ever interpretable?, Tellus B, 61, 361–371, doi:10.1111/j.1600-0889.2008.00401.x, 2009.

Liu, X., Penner, J. E., and Wang, M.: Influence of anthropogenic sulfate and black carbon on upper tropospheric clouds in the NCAR CAM3 model coupled to the IMPACT global aerosol model, J. Geophys. Res., 114, D03204, doi:10.1029/2008JD010492, 2009.

Lohmann, U. and Feichter, J.: Global indirect aerosol effects: a review, Atmos. Chem. Phys., 5, 715–737, doi:10.5194/acp-5-715-2005, 2005.

Lund, M., Berntsen, T., Fuglestvedt, J., Ponater, M., and Shine, K.: How much information is lost by using global-mean climate metrics? An example using the transport sector, Climatic Change, 13, 949–963, doi:10.1007/s10584-011-0391-3, 2011.

Manne, A. S. and Richels, R. G.: An alternative approach to establishing trade-offs among greenhouse gases, Nature, 410, 675–677, 2001.

Manning, M. and Reisinger, A.: Broader perspectives for comparing different greenhouse gases, Proc. Roy. Soc. A, 369, 1891–1905, 2011.

Myhre, G., Highwood, E., Shine, K. P., and Stordal, F.: New estimates of radiative forcing due to well mixed greenhouse gases, Geophys. Res. Lett., 25, 2715–2718, 1998.

Myhre, G., Berglen, T. F., Johnsrud, M., Hoyle, C. R., Berntsen, T. K., Christopher, S. A., Fahey, D. W., Isaksen, I. S. A., Jones, T. A., Kahn, R. A., Loeb, N., Quinn, P., Remer, L., Schwarz, J. P., and Yttri, K. E.: Modelled radiative forcing of the direct aerosol effect with multi-observation evaluation, Atmos. Chem. Phys., 9, 1365–1392, doi:10.5194/acp-9-1365-2009, 2009.

Naik, V., Mauzerall, D., Horowitz, L., Schwarzkopf, M. D., Ramaswamy, V., and Oppenheimer, M.: Net radiative forcing due to changes in regional emissions of tropospheric ozone precursors, J. Geophys. Res., 110, D24306, doi:10.1029/2005jd005908, 2005.

O'Neill, B. C.: The jury is still out on global warming potentials, Climatic Change, 44, 427–443, doi:10.1023/a:1005582929198, 2000.

Olivié, D. J. L. and Peters, G. P.: The impact of model variation in CO_2 and temperature impulse response functions on emission metrics, Earth Syst. Dynam. Discuss., 3, 935–977, doi:10.5194/esdd-3-935-2012, 2012.

Olivié, D. J. L., Peters, G., and Saint-Martin, D.: Atmosphere response time scales estimated from AOGCM experiments, J. Climate, 25, 7956–7972, doi:10.1175/JCLI-D-11-00475.1, 2012.

Penner, J. E., Chen, Y., Wang, M., and Liu, X.: Possible influence of anthropogenic aerosols on cirrus clouds and anthropogenic forcing, Atmos. Chem. Phys., 9, 879–896, doi:10.5194/acp-9-879-2009, 2009.

Pennington, D. W., Potting, J., Finnveden, G., Lindeijer, E., Jolliet, O., Rydberg, T., and Rebitzer, G.: Life cycle assessment part 2: Current impact assessment practice, Environ. Int., 30, 721–739, 2004.

Peters, G. P.: Carbon footprints and embodied carbon at multiple scales, Current Opinion on Environmental Sustainability, 2, 245–250, 2010.

Peters, G., Aamaas, B., Berntsen, T., and Fuglestvedt, F. S.: The integrated global temperature change potential (iGTP) and relationship with other simple emission metrics, Environ. Res. Lett., 6, 044021, doi:10.1088/1748-9326/6/4/044021, 2011a.

Peters, G. P., Aamaas, B., Lund, M. T., Solli, C., and Fuglestvedt, J. S.: Alternative "global warming" metrics in life cycle assessment: A case study with existing transportation data, Environ. Sci. Technol., 45, 8633–8641, doi:10.1021/es200627s, 2011b.

Pinnock, S., Hurley, M. D., Shine, K. P., Wallington, T. J., and Smyth, T. J.: Radiative forcing of climate by hydrochlorofluorocarbons and hydrofluorocarbons, J. Geophys. Res., 100, 23227–23238, doi:10.1029/95jd02323, 1995.

Plattner, G.-K., Knutti, R., Joos, F., Stocker, T. F., von Bloh, W., Brovkin, V., Cameron, D., Driesschaert, E., Dutkiewicz, S., Eby, M., Edwards, N. R., Fichefet, T., Hargreaves, J. C., Jones, C. D., Loutre, M. F., Matthews, H. D., Mouchet, A., Müller, S. A., Nawrath, S., Price, A., Sokolov, A., Strassmann, K. M., and Weaver, A. J.: Long-term climate commitments projected with

climate–carbon cycle models, J. Climate, 21, 2721–2751, 2008.

Prather, M. J.: Lifetimes and eigenstates in atmospheric chemistry, Geophys. Res. Lett., 21, 801–804, doi:10.1029/94GL00840, 1994.

Prather, M. J.: Time scales in atmospheric chemistry: Theory, GWPs for CH_4 and CO, and runaway growth, Geophys. Res. Lett., 23, 2597–2600, doi:10.1029/96GL02371, 1996.

Prather, M. J.: Lifetimes and time scales in atmospheric chemistry, Philosophical Transactions of the Royal Society A: Mathematical, Phys. Eng. Sci., 365, 1705–1726, doi:10.1098/rsta.2007.2040, 2007.

Prather, M. J., Holmes, C. D., and Hsu, J.: Reactive greenhouse gas scenarios: Systematic exploration of uncertainties and the role of atmospheric chemistry, Geophys. Res. Lett., 39, L09803, doi:10.1029/2012gl051440, 2012.

Ramaswamy, V., Boucher, O., Haigh, J., Hauglustaine, D., Haywood, J., Myhre, G., Nakajima, T., Shi, G. Y., Solomon, S., Betts, R., Charlson, R., Chuang, C., Daniel, J. S., Del Genio, A., R., v. D., Feichter, J., Fuglestvedt, J. S., Forster, P., Ghan, S. J., Jones, A., Kiehl, J., Koch, D., Land, C., Lean, J., Lohmann, U., Minschwaner, K., Penner, J. E., Roberts, D. L., Rodhe, H., Roelofs, G. J., Rotstayn, L. D., Schneider, T. L., Schumann, U., Schwartz, S. E., Schwarzkopf, M. D., Shine, K. P., Smith, S., Stevenson, D. S., Stordal, F., Tegen, I., and Zhang, Y.: Radiative forcing of climate change, Climate change 2001: The scientific basis. Contribution of working group i to the third assessment report of the intergovernmental panel on climate change, edited by: Joos, F. and Srinivasan, J., Cambridge University Press, Cambridge, United Kingdom and New York, NY, USA, 2001.

Reisinger, A., Meinshausen, M., Manning, M., and Bodeker, G.: Uncertainties of global warming metrics: CO_2 and CH_4, Geophys. Res. Lett., 37, L14707, doi:10.1029/2010gl043803, 2010.

Reisinger, A., Meinshausen, M., and Manning, M.: Future changes in global warming potentials under representative concentration pathways, Environ. Res. Lett., 6, 024020, doi:10.1088/1748-9326/6/2/024020, 2011.

Reisinger, A., Havlik, P., Riahi, K., Vliet, O., Obersteiner, M., and Herrero, M.: Implications of alternative metrics for global mitigation costs and greenhouse gas emissions from agriculture, Climatic Change, 117, 677–690, doi:10.1007/s10584-012-0593-3, 2013.

Rypdal, K., Rive, N., Berntsen, T., Klimont, Z., Mideksa, T., Myhre, G., and Skeie, R. B.: Costs and global impacts of black carbon abatement strategies, Tellus B, 61, 625–641, 2009.

Samset, B. H. and Myhre, G.: Vertical dependence of black carbon, sulphate and biomass burning aerosol radiative forcing, Geophys. Res. Lett., 38, L24802, doi:10.1029/2011GL049697, 2011.

Shindell, D. T.: Evaluation of the absolute regional temperature potential, Atmos. Chem. Phys., 12, 7955–7960, doi:10.5194/acp-12-7955-2012, 2012.

Shindell, D. and Faluvegi, G.: Climate response to regional radiative forcing during the twentieth century, Nat. Geosci., 2, 294–300, 2009.

Shindell, D. T., Faluvegi, G., Koch, D. M., Schmidt, G. A., Unger, N., and Bauer, S. E.: Improved attribution of climate forcing to emissions, Science, 326, 716–718, doi:10.1126/science.1174760, 2009.

Shindell, D., Kuylenstierna, J. C. I., Vignati, E., van Dingenen, R., Amann, M., Klimont, Z., Anenberg, S. C., Muller, N., Janssens-Maenhout, G., Raes, F., Schwartz, J., Faluvegi, G., Pozzoli, L., Kupiainen, K., Höglund-Isaksson, L., Emberson, L., Streets, D., Ramanathan, V., Hicks, K., Oanh, N. T. K., Milly, G., Williams, M., Demkine, V., and Fowler, D.: Simultaneously mitigating near-term climate change and improving human health and food security, Science, 335, 183–189, doi:10.1126/science.1210026, 2012.

Shine, K. P.: The global warming potential – the need for an interdisciplinary retrail, Climatic Change, 96, 467–472, 2009.

Shine, K. P., Berntsen, T. K., Fuglestvedt, J. S., and Sausen, R.: Scientific issues in the design of metrics for inclusion of oxides of nitrogen in global climate agreements, Proc. Natl. Acad. Sci. USA, 102, 15768–15773, doi:10.1073/pnas.0506865102, 2005a.

Shine, K. P., Fuglestvedt, J. S., Hailemariam, K., and Stuber, N.: Alternatives to the global warming potential for comparing climate impacts of emissions of greenhouse gases, Climatic Change, 68, 281–302, doi:10.1007/s10584-005-1146-9, 2005b.

Shine, K. P., Berntsen, T., Fuglestvedt, J. S., Stuber, N., and Skeie, R. B.: Comparing the climate effect of emissions of short and long lived climate agents, Philos. Trans. Roy. Soc. A, 365, 1903–1914, 2007.

Skeie, R. B., Berntsen, T. K., Myhre, G., Tanaka, K., Kvalevåg, M. M., and Hoyle, C. R.: Anthropogenic radiative forcing time series from pre-industrial times until 2010, Atmos. Chem. Phys., 11, 11827–11857, doi:10.5194/acp-11-11827-2011, 2011.

Skodvin, T. and Fuglestvedt, J. S.: A comprehensive approach to climate change: Political and scientific considerations, Ambio, 26, 351–358, 1997.

Smith, S. J. and Wigley, T. M. L.: Global warming potentials: 2. Accuracy, Climatic Change, 44, 459–469, doi:10.1023/a:1005537014987, 2000a.

Smith, S. J. and Wigley, T. M. L.: Global warming potentials: 1. Climatic implications of emissions reductions, Climatic Change, 44, 445–457, 2000b.

Smith, S. M., Lowe, J. A., Bowerman, N. H. A., Gohar, L. K., Huntingford, C., and Allen, M. R.: Equivalence of greenhouse-gas emissions for peak temperature limits, Nat. Clim. Change, 2, 535–538, doi:10.1038/NCLIMATE1496, 2012.

Stevenson, D. S., Doherty, R. M., Sanderson, M. G., Collins, W. J., Johnson, C. E., and Derwent, R. G.: Radiative forcing from aircraft NO_x emissions: Mechanisms and seasonal dependence, J. Geophys. Res., 109, D17307, doi:10.1029/2004jd004759, 2004.

Tanaka, K., O'Neill, B. C., Rokityanskiy, D., Obersteiner, M., and Tol, R. S. J.: Evaluating global warming potentials with historic temperature, Climatic Change, 96, 113–466, 2009.

Tanaka, K., Peters, G. P., and Fuglestvedt, J. S.: Multi-component climate policy: Why do emission metrics matter?, Carbon Management, 1, 191–197, 2010.

Tanaka, K., Berntsen, T., Fuglestvedt, J. S., and Rypdal, K.: Climate effects of emission standards: The case for gasoline and diesel cars, Environ. Sci. Technol., 46, 5205–5213, doi:10.1021/es204190w, 2012.

Tol, R. S. J., Berntsen, T., O'Neill, B. C., Fuglestvedt, J. S., and Shine, K.: A unifying framework for metrics for aggregating the climate effect of different emissions, Environ. Res. Letts., 7, 044006, doi:10.1088/1748-9326/7/4/044006, 2012.

Victor, D. G.: Calculating greenhouse budgets, in: Nature, Scientific Correspondence, p. 431, 1990.

Voulgarakis, A., Naik, V., Lamarque, J.-F., Shindell, D. T., Young, P. J., Prather, M. J., Wild, O., Field, R. D., Bergmann, D., Cameron-Smith, P., Cionni, I., Collins, W. J., Dalsøren, S. B., Doherty, R. M., Eyring, V., Faluvegi, G., Folberth, G. A., Horowitz, L. W., Josse, B., MacKenzie, I. A., Nagashima, T., Plummer, D. A., Righi, M., Rumbold, S. T., Stevenson, D. S., Strode, S. A., Sudo, K., Szopa, S., and Zeng, G.: Analysis of present day and future OH and methane lifetime in the ACCMIP simulations, Atmos. Chem. Phys., 13, 2563–2587, doi:10.5194/acp-13-2563-2013, 2013.

Warren, S. G., and Wiscombe, W. J.: A model for the spectral albedo of snow. II: Snow containing atmospheric aerosols, J. Atmos. Sci., 37, 2734–2745, doi:10.1175/1520-0469(1980)037<2734:AMFTSA>2.0.CO;2, 1980.

Wigley, T. M. L.: A simple inverse carbon cycle model, Global Biogeochem. Cy., 5, 373–382, doi:10.1029/91gb02279, 1991.

Wigley, T. M. L.: The Kyoto protocol: CO_2 CH_4 and climate implications, Geophys. Res. Lett., 25, 2285–2288, doi:10.1029/98GL01855, 1998.

Wigley, T. M. L., Smith, S. J., and Prather, M. J.: Radiative forcing due to reactive gas emissions, J. Climate, 15, 2690–2696, doi:10.1175/1520-0442(2002)015<2690:RFDTRG>2.0.CO;2, 2002.

Wild, O., Prather, M. J., and Akimoto, H.: Indirect long-term global radiative cooling from NO_x emissions, Geophys. Res. Lett., 28, 1719–1722, doi:10.1029/2000gl012573, 2001.

WMO: Scientific assessment of ozone depletion: 1998, global ozone research and monitoring project, report no. 44, World Meteorological Organization, Geneva, Switzerland, 1999.

Wuebbles, D. J.: Beyond CO_2 – the other greenhouse gases, UCRL-99883, Air and waste management association paper 89-119.4, Livermore National Laboratory, 1989.

Wuebbles, D. J., Jain, A. K., Patten, K. O., and Grant, K. E.: Sensitivity of direct global warming potentials to key uncertainties, Climatic Change, 29, 265–297, doi:10.1007/bf01091865, 1995.